Synthesis, Biological Evaluation, and Molecular Modeling of Ribose-Modified Adenosine Analogues as Adenosine Receptor Agonists

Loredana Cappellacci,[†] Palmarisa Franchetti,[†] Michela Pasqualini,[†] Riccardo Petrelli,[†] Patrizia Vita,[†] Antonio Lavecchia,[⊥] Ettore Novellino,[⊥] Barbara Costa,[‡] Claudia Martini,[‡] Karl-Norbert Klotz,[§] and Mario Grifantini*[,†]

Dipartimento di Scienze Chimiche, Università di Camerino, 62032 Camerino, Italy, Dipartimento di Chimica Farmaceutica e Tossicologica, Università di Napoli "Federico II", 80131 Napoli, Italy, Dipartimento di Neurobiologia, Farmacologia e Biotecnologia, Università di Pisa, 56126 Pisa, Italy, and Institut für Pharmakologie und Toxikologie, Universität Würzburg, D-97078 Würzburg, Germany

Received July 24, 2004

A number of 3′-*C*-methyl analogues of selective adenosine receptor agonists such as CPA, CHA, CCPA, 2′-Me-CCPA, NECA, and IB-MECA was synthesized to further investigate the subdomain of the receptor that binds the ribose moiety of the ligands. Affinity data at A_1, A_{2A}, and A_3 receptors in bovine brain membranes showed that the 3′-*C*-modification in adenosine resulted in a decrease of the affinity at all three receptor subtypes. When this modification was combined with N^6-substitution with groups that induce high potency and selectivity at A_1 receptor, the affinity and selectivity were increased. However, all 3′-*C*-methyl derivatives proved to be very less active than the corresponding 2′-*C*-methyl analogues. The most active compound was found to be 3′-Me-CPA which displayed a K_i value of 0.35 μM at A_1 receptor and a selectivity for A_1 vs A_{2A} and A_3 receptors higher than 28-fold. 2′-Me-CCPA was confirmed to be the most selective, high affinity agonist so far known also at human A_1 receptor with a K_i value of 3.3 nM and 2903- and 341-fold selective vs human A_{2A} and A_3 receptors, respectively. In functional assay, 3′-Me-CPA, 3′-Me-CCPA, and 2-Cl-3′-Me-IB-MECA inhibited forskolin-stimulated adenylyl cyclase activity with IC_{50} values ranging from 0.3 to 4.9 μM, acting as full agonists. A rhodopsin-based model of the bovine A_1AR was built to rationalize the higher affinity and selectivity of 2′-*C*-methyl derivatives of N^6-substituted-adenosine compared to that of 3′-*C*-methyl analogues. In the docking exploration, it was found that 2′-Me-CCPA was able to form a number of interactions with several polar residues in the transmembrane helices TM-3, TM-6, and TM-7 of bA_1AR which were not preserved in the molecular dynamics simulation of 3′-Me-CCPA/bA_1AR complex.

Introduction

Adenosine modulates a great variety of physiological functions mediated by different subtypes of G protein-coupled receptors. Many efforts have been made to develop therapeutic agents based on selective interactions with one of the four adenosine receptor subtypes A_1, A_{2A}, A_{2B}, and A_3 (ARs).[1] Activation of these receptors inhibits or stimulates the intracellular enzyme adenylate cyclase (AC). A_1 and A_3 receptors are coupled to the inhibitory G-protein Gi/Go. Recent studies have pointed out that A_1 receptors are also coupled in atrial cardiac myocytes to other effectors such as calcium or potassium ion channels and phospholipase C (PLC), while A_3 receptors are also coupled to both PLC and phospholipase D (PLD). A_{2A} and A_{2B} receptors are coupled to the stimulatory Gs protein, thus stimulating AC activity. A_{2B} is also coupled to PLC. In recent years it has become more and more clear that adenosine receptors may be targets for the development of new drugs. Among the pathological conditions that might be treated with agonists or antagonists of adenosine receptors there are Parkinson's disease, hypoxia/ischemia, epilepsy, kidney disease, asthma and cancer.[2] A beneficial therapeutic effect of adenosine A_1 receptor agonists for type II diabetic patients was also suggested.[3] Most of the agonists of adenosine receptors so far known are adenosine derivatives;[1] only recently have A_{2B} non-adenosine agonists been reported.[4] Structure−activity relationship studies have pointed out that the ribose recognition domain of adenosine and adenosine analogues contributes strongly to the affinity for adenosine receptors. Among ribose modifications, replacement of hydrogen atoms of the ribose ring with a methyl group in adenosine and adenosine analogues afforded compounds with various affinity and selectivity.[5,6] We have reported that the introduction of a methyl group at the *C*-2′ position in adenosine resulted in a decrease of affinity, particularly at A_{2A} and A_3 ARs.[5] However, when this modification was combined with N^6-substitution with groups that induce high potency and selectivity at the A_1 receptor, the selectivity for A_1 vs A_{2A} and A_3 ARs was increased. So, 2′-Me-CCPA,[5] the 2′-*C*-methyl analogue of 2-chloro-N^6-cyclopentyladenosine (CCPA),[7] proved to be a potent and highly selective agonist at bovine A_1AR with A_3/A_1 selectivity higher than that of CCPA (2′-Me-CCPA A_3/A_1 selectivity = 2856, CCPA A_3/

* To whom correspondence should be addressed. Phone: +39-0737-402233. Fax +39-0737-637345. E-mail: mario.grifantini@unicam.it.
[†] Università di Camerino.
[⊥] Università di Napoli "Federico II".
[‡] Università di Pisa.
[§] Universität Würzburg.

10.1021/jm049408n CCC: $30.25
Published on Web 02/05/2005

Chart 1. Chemical Structures of Reported 2′- and 3′-*C*-Methyl-adenosine Derivatives

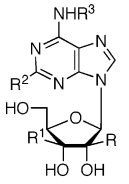

1 R = CH_3; R^1, R^2 = H; R^3 = cyclohexyl
2 R = CH_3; R^1, R^2 = H; R^3 = benzyl
3 R = CH_3; R^1 = H; R^2 = Cl; R^3 = 3-iodobenzyl
4 R, R^2 = H; R^1 = CH_3; R^3 = cyclopentyl
5 R, R^2 = H; R^1 = CH_3; R^3 = cyclohexyl
6 R, R^2 = H; R^1 = CH_3; R^3 = benzyl
7 R, R^2 = H; R^1 = CH_3; R^3 = 3-iodobenzyl
8 R = H; R^1 = CH_3; R^2 = Cl; R^3 = cyclopentyl
9 R = H; R^1 = CH_3; R^2 = Cl; R^3 = 3-iodobenzyl

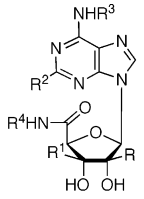

14 R, R^2 = H; R^1 = CH_3; R^3 = H; R^4 = C_2H_5
15 R, R^2 = H; R^1 = CH_3; R^3 = 3-iodobenzyl; R^4 = CH_3
25 R = CH_3; R^1 = H; R^2 = Cl; R^3 = 3-iodobenzyl; R^4 = CH_3
26 R = H; R^1 = CH_3; R^2 = Cl; R^3 = 3-iodobenzyl; R^4 = CH_3
27 R = CH_3; R^1 = H; R^2 = $NHCH_3$; R^3 = 3-iodobenzyl; R^4 = CH_3
28 R = H; R^1 = CH_3; R^2 = $NHCH_3$; R^3 = 3-iodobenzyl; R^4 = CH_3

A_1 selectivity = 87). On the other hand, we found that the 1′-*C*-methyl modification in N^6-substituted adenosine analogues decreased the affinity, particularly at A_1 and A_{2A} ARs.[6]

The potential clinical applications of selective A_1/A_3 agonists as cardioprotective and neuroprotective agents prompted us to further investigate the receptor subdomain that binds the ribose moiety by the study of 3′-*C*-methyl derivatives of N^6-substituted adenosine and 2-chloroadenosine. The present paper reports on the synthesis and binding studies of these compounds as well as of novel di- and trisubstituted analogues of 2′-*C*-methyladenosine. Furthermore, 3′-*C*-methyl derivatives of the A_3AR selective agonist IB-MECA (N^6-(3-iodobenzyl)-adenosine-5′-*N*-methyluronamide), and of its even more selective 2-chloro (2-Cl-IB-MECA) and 2-methylamino derivatives,[8] were synthesized to investigate the role of the conformation of these nucleosides in binding to adenosine receptors. The 3′-*C*-methyl analogue of NECA (adenosine-5′-*N*-ethyluronamide) was also synthesized (Chart 1).

Chemistry

3′-*C*-Methyl adenosine N^6-substituted and N^6/*C*-2 disubstituted derivatives and novel 2′-*C*-methyl analogues were synthesized as reported in Scheme 1. Nucleophilic displacement of the 6-chlorine atom in the protected compounds **10**, **11**[5] and **12**, **13**[9] with cyclopentylamine, cyclohexylamine, benzylamine, or 3-iodobenzylamine in anhydrous ethanol gave, after deprotection with methanolic ammonia, the corresponding N^6-substituted nucleosides **1**−**9**. The assignment of the β-anomeric structure of these compounds was performed by proton NOE data.

3′-*C*-Methyl derivatives of NECA (**14**) and IB-MECA (**15**) were also obtained (Scheme 2). 2′,3′-Isopropylidene derivatives of compounds **16** and **21** (**17** and **22**, respectively) were oxidized by the TEMPO (2,2,6,6-tetramethylpiperidin-1-yloxy) BAIB (diacetoxyiodo-benzene) system[10] in a 1:1 acetonitrile−water solvent to give the corresponding 5′-carboxylic acids **18** and **23**. We preferred to use the TEMPO−BAIB system because this is a mild and efficient method that allows the synthesis of 5′-carboxylic acid nucleosides in high yield with a short reaction time. Compounds **18** and **23** were converted into ethyl esters **19** and **24**, respectively, by

Scheme 1[a]

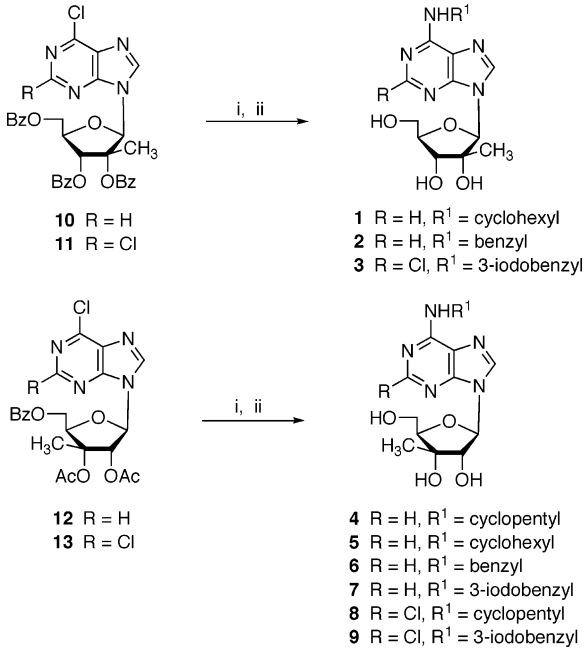

10 R = H
11 R = Cl

1 R = H, R^1 = cyclohexyl
2 R = H, R^1 = benzyl
3 R = Cl, R^1 = 3-iodobenzyl

12 R = H
13 R = Cl

4 R = H, R^1 = cyclopentyl
5 R = H, R^1 = cyclohexyl
6 R = H, R^1 = benzyl
7 R = H, R^1 = 3-iodobenzyl
8 R = Cl, R^1 = cyclopentyl
9 R = Cl, R^1 = 3-iodobenzyl

[a] Reagents and conditions: (i) cyclopentylamine, cyclohexylamine, or benzylamine, EtOH, Δ, or 3-iodobenzylamine hydrochloride, TEA, EtOH, Δ; (ii) NH_3/MeOH, rt.

reaction with $SOCl_2$ and anhydrous ethanol at room temperature. Displacement of the 6-chlorine atom of **19** with 3-iodobenzylamine and treatment of intermediate **20** with methylamine followed by deprotection with 90% formic acid gave 3′-Me-IB-MECA (**15**). In the same way, compound **24** was converted into 3′-Me-NECA (**14**) by reaction with ethylamine.

The synthesis of 2-Cl-2′-Me-IB-MECA (**25**), 2-Cl-3′-Me-IB-MECA (**26**), 2-methylamino-2′-Me-IB-MECA (**27**), and 2-methylamino-3′-Me-IB-MECA (**28**) was carried out as described in Scheme 3. Compounds **3** and **7** were protected as 2′,3′-*O*-isopropylidene derivatives (**29** and **32**, respectively) by reaction with 2,2-dimethoxypropane, camphorsulfonic acid in acetone. Oxidation of **29** and **32** with the TEMPO−BAIB system gave the corresponding 5′-carboxylic acids **30** and **33**, respectively. The ethyl esters **31** and **34**, obtained from **30** and **33** as described for **19** and **24**, were converted into nucleosides **25** and **26**, respectively, by treatment with methylamine

Scheme 2[a]

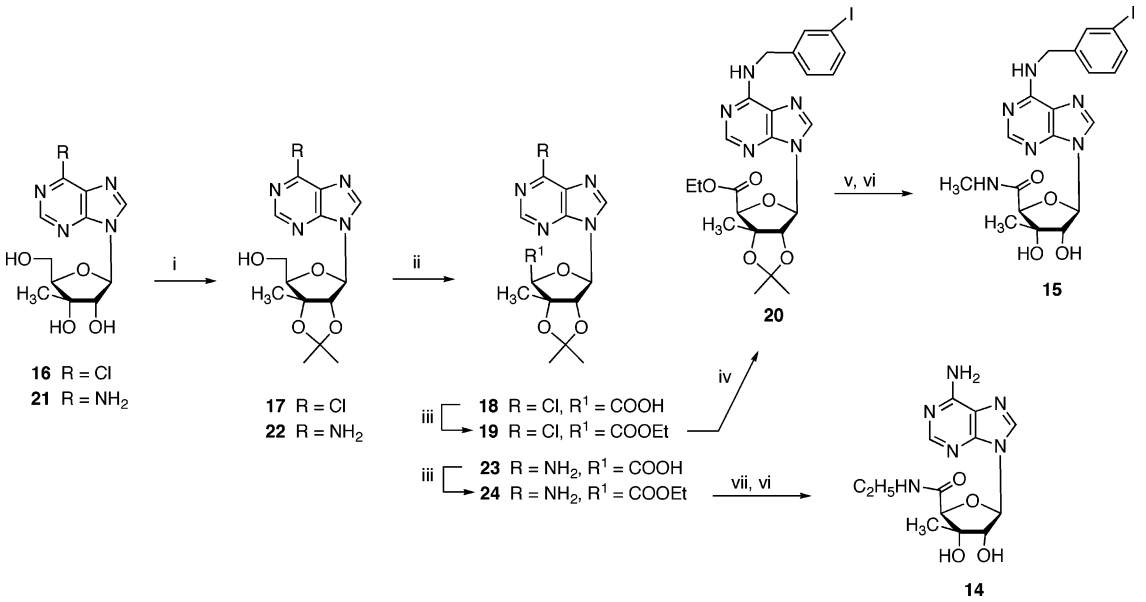

[a] Reagents and conditions: (i) 2,2-dimethoxypropane, camphorsulfonic acid, acetone, Δ; (ii) TEMPO−BAIB, MeCN/H_2O (1:1), rt; (iii) $SOCl_2$, EtOH, rt; (iv) 3-iodobenzylamine hydrochloride, TEA, EtOH; (v) CH_3NH_2, −20 °C to rt; (vi) 90% HCOOH, Δ; (vii) $C_2H_5NH_2$.

Scheme 3[a]

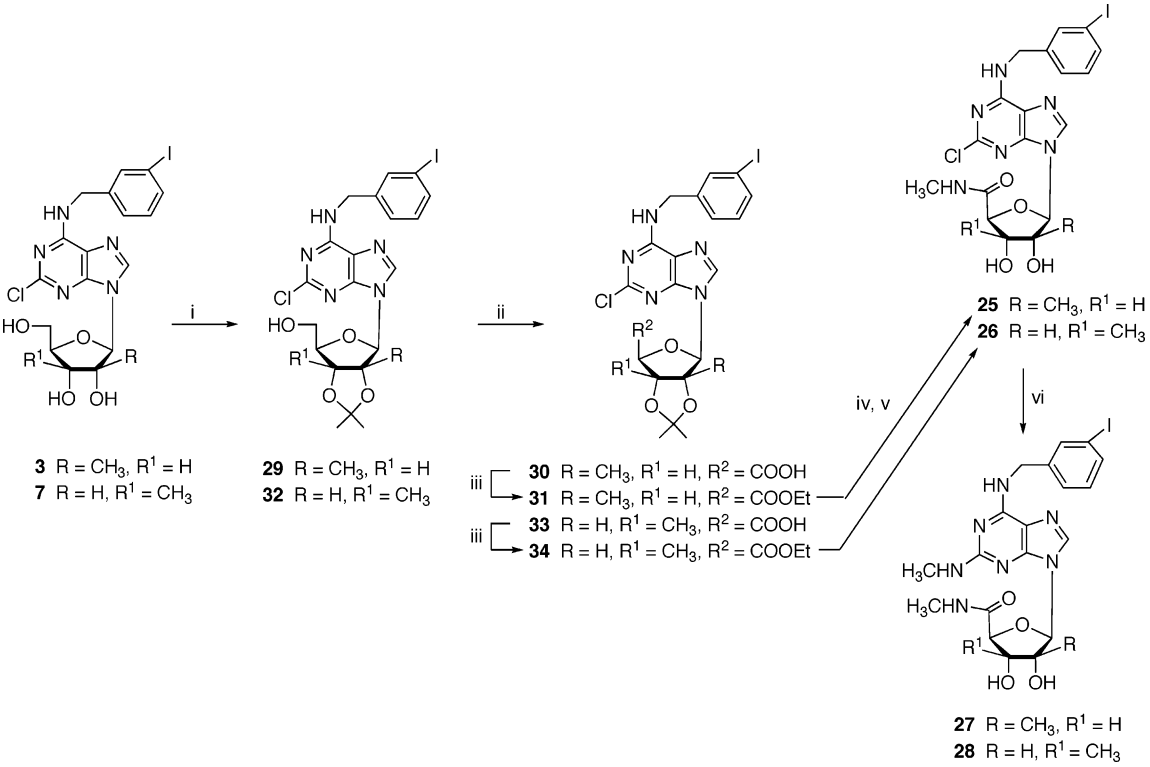

[a] Reagents and conditions: (i) 2,2-dimethoxypropane, camphorsulfonic acid, acetone, Δ; (ii) TEMPO−BAIB, MeCN/H_2O (1:1), rt; (iii) $SOCl_2$, EtOH, rt; (iv) CH_3NH_2, −20 °C to rt; (v) 90% HCOOH, Δ; (vi) 2 N CH_3NH_2/THF, Δ.

and then deisopropylidenation. Displacement of 2-chlorine atom of compounds **25** and **26** with methylamine gave **27** and **28**, respectively.

2′-Me-Ado, 3′-Me-Ado, 2-Cl-2′-Me-Ado, 2′-Me-CPA, 2′-Me-CCPA, 2′-Me-IB-Ado, 2′-Me-NECA, and 2′-Me-IB-MECA were prepared according to known procedures as reference compounds for biological evaluation.[5,11]

Information concerning the predominant solution conformation of synthesized 3′-*C*-methyl adenosine derivatives was obtained via ^{1}H NMR and NOE experiments. When anomeric proton of compounds **4**-**9**, **14**, **15**, **26**, and **28** was irradiated, an enhancement of the H-8 signal was observed, indicating that a population of syn conformers is present in these compounds. However, because the H-8 enhancement in **14**, **15**, and **26** (about 6.3%) is lower than that observed in NECA (22%), the conformation of 3′-Me-NECA (**14**), 3′-Me-IB-MECA (**15**), and 2-Cl-3′-Me-IB-MECA (**26**) should diverge slightly from those of the nonmethylated analogues. On the basis of the correlation reported by Rosemeyer et al.,[12]

Table 1. Affinity of 2′-, and 3′-*C*-Methyl-adenosine Derivatives in Radioligand Assays at Bovine Cortical Membranes (A_1 and A_3) and Bovine Brain Striatum (A_{2a}) Receptors[a−c]

		K_i (nM) or % displacement at 10^{-5} M					
compd no.	compd label	A_1[a]	A_{2A}[b]	A_3[c]	A_{2A}/A_1	A_3/A_1	A_{2A}/A_3
1	2′-Me-CHA	30 ± 3.1	28%	2560 ± 238	>333	85.3	>3.9
2	2′-Me-B-Ado	460 ± *51*	40%	670 ± 65	>21.7	1.4	>14.0
3	2-Cl-2′-Me-IB-Ado	85 ± 7.8	470 ± 44	163 ± 17	5.5	1.9	2.68
4	3′-Me-CPA	350 ± 38	2%	30%	>28.6	>28.6	
5	3′-Me-CHA	22%	0%	0%			
6	3′-Me-B-Ado	23%	21%	15%			
7	3′-Me-IB-Ado	30%	0%	10%			
8	3′-Me-CCPA	5370 ± 611	17%	20%	>1.9		
9	2-Cl-3′-Me-IB-Ado	4300 ±407	3200 ± 345	2700 ± 282	0.74	0.62	1.18
14	3′-Me-NECA	6%	0%	28%			
15	3′-Me-IB-MECA	5620 ± 570	5%	3210 ± 306	>1.78	0.57	
25	2-Cl-2′-Me-IB-MECA	325 ± 37	2780 ± 264	480 ± 44	8.55	1.48	5.79
26	2-Cl-3′-Me-IB-MECA	4530 ±452	15%	5780± 576	>2.21	1.27	
27	2-MeNH-2′-Me-IB-MECA	8%	0%	12%			
28	2-MeNH-3′-Me-IB-MECA	1310 ± 128	4000 ± 411	1200 ± 123	3.05	0.92	3.33
	2′-Me-Ado	1120 ± 80	5800 ± 950	0%	5.2	>8.9	>0.58
	3′-Me-Ado	13%	4%	0%			
	2-Cl-2′-Me-Ado	350 ± 40	4890 ± 850	7%	13.9	>28.5	<0.49
	2′-Me-CPA	10 ± 1.5	7560 ± 735	220 ± 23	756	22	34.3
	2′-Me-CCPA	3 ± 0.6	4560 ± 850	8570 ± 848	1520	2856	0.53
	IB-Ado	23:t 2	121 + 10	15.2 ± 2	5.3	0.66	7.96
	2′-Me-IB-Ado	50 ± 4.1	680 ± 58	65 ± 61	13.6	1.3	10.5
	NECA	14 ± 4	16 ± 3	73 ± 5	1.14	5.2	0.22
	2′-Me-NECA	770 ± 65	220 ± 23	420 ± 38	0.28	0.54	0.52
	IB-MECA	12 ± 2	40 ± 4	8.8 ± 0.9	3.33	073	4.54
	2-Cl−IB-MECA	890 ± 61	401 ± 25	0.22 ± 0.02	0.45	0.00025	1822.7
	2′-Me-IB-MECA	350 ± 38	1260 ± 131	240 ± 25	3.6	0.68	5.25

[a] Displacement of specific [^{3}H]DPCPX binding in bovine cortical membranes expressed as K_i ± SEM in nM ($n = 3$). [b] Displacement of specific [^{3}H]CGS21680 binding in bovine striatal membranes expressed as K_i ± SEM in nM ($n = 3$). [c] Competition assay of [^{125}I]-N^6-(3-iodo-4-aminobenzyl)-5′-*N*-methylcarboxamido-adenosine ([^{125}I]AB-MECA) to bovine cortical membranes in the presence of the A_1AR selective antagonist DPCPX (20 nM); the residual binding which was not displaced by DPCPX represented binding to A_3AR.

the observed H-1′ enhancement translates into a 60% population of the syn conformer. Information concerning the solution conformation of the ribosyl moiety of these nucleosides was obtained by the coupling constant values. The 3′-*C*-substitution precludes getting information from $J_{2'3'}$ and $J_{3'4'}$ values, leaving only $J_{1'2'}$ as a clue to sugar puckering. It was found that the $J_{1'2'}$ value of compounds **4**−**9**, **14**, **15**, **26**, and **28** is in the range of 7.7−8.2 Hz, indicating that they are predominantly *S*-puckered.

Biological Evaluation

Ribose-modified nucleosides **1**-**9** and NECA and IB-MECA analogues (**14**, **15**, and **25**−**28**) were evaluated in radioligand binding assays to determine their affinity at A_1, A_{2A}, and A_3 ARs (Table 1). In particular, affinities for A_1 and A_{2A} receptors were determined in competition assays in bovine cortical membranes (A_1) and bovine brain striatum (A_{2A}) using, respectively, [^{3}H]DPCPX (1,3-dipropyl-8-cyclopentylxanthine) and [^{3}H]CGS21680 (2-[4-(2-carboxyethyl)phenyl]ethyl-amino-5′-*N*-ethylcarboxamido-adenosine) as radioligands.[13,14] Affinity for A_3AR was determined in competition assays of [^{125}I]AB-MECA ([^{125}I]-N^6-(3-iodo-4-aminobenzyl)-5′-*N*-methylcarboxamido-adenosine) to bovine cortical membranes in the presence of the A_1AR selective antagonist DPCPX (20 nM);[14] the residual binding which was not displaced by DPCPX represented binding to A_3AR. 2′-Me-Ado, 3′-Me-Ado, 2-Cl-2′-Me-Ado, 2′-Me-CPA, 2′-Me-CCPA, IB-Ado, 2′-Me-IB-Ado, NECA, 2′-Me-NECA, IB-MECA, 2-Cl-IB-MECA, and 2′-Me-IB-MECA were used as reference compounds. Introduction of a methyl group in the adenosine 3′-position proved to be not tolerated, while 2′-methyl modification confirmed A_1 selectivity vs A_{2A} and A_3 receptors. We ascribed the different affinity of 2′-Me-Ado and 3′-Me-Ado to the different conformation of the furanose ring of these nucleosides in solution (North ($^3T_2$)-anti and South ($^2T_3$)-syn, respectively).[5] The 3′-*C*-methyl-substituted adenosine analogues **4**−**9** showed a marked preference for the South ($^2T_3$)-syn conformation as determined by ^{1}H NMR data.

N^6-Substitution with a cyclopentyl group in 3′-Me-Ado increased the affinity at A_1AR (K_i = 0.35 μM), restoring A_1 selectivity. 3′-Me-CPA proved to be the most active and selective compound at A_1AR among the 3′-*C*-methyl-N^6-substituted adenosine analogues reported in this study. Introduction of a chlorine atom in the 2-position of 3′-Me-CPA (3′-Me-CCPA, **8**) induced a 15-fold decrease of the affinity at A_1AR. This is a surprising result because a similar substitution in 2′-Me-CPA (2′-Me-CCPA) brings about an increase of both affinity and selectivity at this receptor subtype. 2′-Me-CCPA was confirmed to be a potent agonist and the most selective one at bovine A_1AR known so far. This compound proved to be a potent A_1 agonist also versus human adenosine receptor (Table 2), with a 2903-fold and 341-fold selectivity vs A_{2A} and A_3 ARs, respectively.

N^6-Substitution of 3′-Me-Ado with a benzyl or 3-iodobenzyl group did not increase the affinity at bovine ARs; however, the introduction of a chlorine in the 2-position of 3′-Me-IB-Ado to give 2-Cl-3′-Me-IB-Ado (**9**) conferred a better affinity at A_1/ A_{2A}/A_3 receptors.

With regard to the novel 2′-*C*-methyl-N^6-substituted adenosine analogues (compounds **1**-**3**), the introduction of a cyclohexyl group (2′-Me-CHA, **1**) resulted in a good affinity at A_1AR with a selectivity vs A_{2A} and A_3 ARs of

Table 2. Binding Affinity of 2′-Me-CCPA and CCPA at Human A_1, A_{2A}, A_{2B}, A_3 Adenosine Receptor Subtypes Expressed in CHO Cells

	K_i (nM)						
compd	A_1	A_{2A}	A_{2B}[a]	A_3	A_{2A}/A_1	A_3/A_1	A_{2A}/A_3
2′-Me-CCPA	3.3	9580	37600	1150	2903	341	8.3
CCPA	0.8	2300	18800	42	2875	53	55

[a] EC_{50} values (nM) are reported for the agonist-mediated stimulation of adenylyl cyclase activity in a membrane preparation.

>333- and 85.3-fold, respectively. N^6-Benzyl substitution in 2′-Me-Ado (compound **2**) resulted in moderate affinity at A_1 and A_3 ARs but low selectivity, while the introduction of a chlorine atom at the 2-position of 2′-Me-IB-Ado (compound **3**) reduced both A_1 and A_3 affinity.

In the case of the adenosine 5′-uronamide analogues **14**, **15**, **25**-**28**, introduction of a methyl group in the 2′- or 3′-position brought about a decrease of affinity at all three receptor subtypes as compared to NECA and IB-MECA. 2′-Me-NECA (K_i values in the range of 0.22−0.77 μM) resulted 55-fold less active than NECA at A_1, 13.7-fold at A_{2A}, and 5.7-fold at A_3AR. 2′-Me-IB-MECA proved to be less potent than IB-MECA with K_i values ranging from 0.24 to 1.2 μM, and a moderate selectivity for A_3AR. On the contrary, the 2′-*C*-methyl modification in 2-Cl-IB-MECA (compound **25**) resulted in increased affinity at A_1 receptor (2.7-fold) but reduced affinity at A_{2A} and A_3 ARs (6.9- and 2180-fold, respectively).

A methyl group in the 3′-position of NECA (compound **14**) is not tolerated at all three receptor subtypes. As found in the case of rat and human adenosine receptors, N^6-substitution of MECA with a 3-iodobenzyl group (IB-MECA) increased the affinity, in particular at A_3 and A_1 receptors. However, when this modification was combined with the introduction of a methyl group in the 3′-position of the ribose moiety (compound **15**), both affinity and selectivity were decreased. Finally, the 2-substitution in 3′-Me-IB-MECA with a chlorine atom (compound **26**) did not improve the affinity at A_3AR, while an analogous substitution in IB-MECA increased the affinity of 40-fold at this receptor subtype. Introduction in 2-position of a methylamino group gave rise to a different result. In fact, the 2′-*C*-methyl derivative **27** was devoid of affinity, while 3′-*C*-methyl isomer **28** showed low affinity at all three receptor subtypes.

Compounds **3**, **4**, **8**, **25**, and **26** were also tested in a functional assay at A_1 receptors in rat cortical membranes for their ability to inhibit forskolin-stimulated adenylyl cyclase. The efficacy of these compounds was compared with that obtained for CHA, a selective A_1 adenosine receptor agonist (Table 3, and Figure 1 of the Supporting Information). CHA proved to be the most potent inhibitor (IC_{50} 1.41 nM) with a maximal inhibitory effect of 16.2% similar to that of the other compounds (values ranging from 17.8 to 22%). Compounds **3** (2-Cl-2′-Me-IB-Ado), **4** (3′-Me-CPA), and **25** (2-Cl-2′-Me-IB-MECA) showed the highest IC_{50} values (102, 304, and 279 nM, respectively) among the novel compounds. Finally, although compounds **8** (3′-Me-CCPA) and **26** (2-Cl-3′-Me-IB-MECA) showed lower IC_{50} values (4010 and 4908 nM, respectively), they achieved the maximal efficacy. Thus, in the functional assay all compounds tested behave as full agonists for A_1AR.

Table 3. Inhibition of Adenylyl Cyclase Activity in Rat Cortical Membranes by Compounds **3**, **4**, **8**, **25**, and **26**[a]

compd	IC_{50} (nM)	% maximal inhibition
CHA	1.41 ± 0.7	16.2 ± 2.2
3	102 ± 9	22.0 ± 1.3
4	304 ± 20	18.1 ± 1.0
8	4010 ± 360	21.8 ± 1.3
25	279 ± 24	19.3 ± 1.0
26	4908 ± 470	17.8 ± 1.0

[a] IC_{50} values and the maximal inhibitory effects were obtained from nonlinear curve fitting of data using GraphPad computer program. All values are the mean ± SEM of three independent experiments

Molecular Modeling. The above-discussed SARs do not allow us to establish whether both 2′-*C*-methyl and 3′-*C*-methyl derivatives of N^6-substituted adenosine interact with the bA_1AR recognition site with a similar or different binding mode. So, a computational study was performed to elucidate the hypothetical binding mode of 2′-Me-CCPA and 3′-Me-CCPA, which show a different activity profile, and to interpret our experimental results.

The bovine A_1AR (bA_1AR) model used for this purpose included the seven transmembrane helical domains (TMs) and was built in homology with the recently published X-ray structure of bovine rhodopsin.[15] Details of the model building are given in the Experimental Section. To determine the most favorable binding locations and orientations for the above-mentioned compounds, we used the automated docking program AutoDock.[16] The 50 independent docking runs carried out for each ligand generally converged to a small number of different positions ("clusters" of results differing by less than 1.5 Å rmsd). Generally, the top clusters (i.e. those with the most favorable ΔG_{bind}) were also associated with the highest frequency of occurrence, which suggests a good convergence behavior of the search algorithm. The best results in terms of free energy of binding were all located in a similar position at the active site. The most important interactions found for each compound are summarized in Table 4.

For each of the ribose-modified ligands (2′-Me-CCPA and 3′-Me-CCPA), very clear preference for a single position in the binding site could be obtained. Interestingly, both results were located in the cavity between TM3, TM5, TM6, and TM7 and involved essentially the same residues, but playing different roles in agonist binding in each case. For 2′-Me-CCPA, the result with top binding energy (−12.0 kcal/mol) was found 19 times out of 50. The N^6 amino group of the ligand formed a hydrogen bond with the CO oxygen of Asn254. The ribose moiety was coordinated to several hydrophilic residues in TM3 and TM7. In particular, the 2′-OH, 3′-OH, and 5′-OH groups of the ribose ring were involved in hydrogen bonding with the N^{δ} imidazole nitrogen of His278 (TM7) and the OH oxygen of Thr91 (TM3), respectively. Moreover, the ribose O-4′ oxygen was engaged in a hydrogen bond with the OH hydrogen of Thr91. A very similar binding position was also observed for compound 3′-Me-CCPA (ΔG of −11.9 kcal/mol, found 25 times out of 50). However, in this case, no hydrogen bonds involving the ribose moiety were observed, and only a single interaction was achieved, between the 5′-OH and the Ser277 side chain. Moreover, it is worth noting that the N^6 amino group of the ligand was

Table 4. Result of 50 Independent Docking Runs for Each Ligand[a]

ligand	N_{tot}	f_{occ}	ΔG_{bind}	surrounding residues
2′-Me-CCPA	10	19	−12.3	Ala84 (TM3), Val87 (TM3), Leu88 (TM3), Ilel89 (TM3), **Thr91** (TM3), Gln92 (TM3), Met180 (TM5), Val181 (TM5), Asn184 (TM5), Phe243 (TM6), Ser246 (TM6), Trp247 (TM6), Leu250 (TM6), His251 (TM6), **Asn254** (TM6), Thr257 (TM6), Ile270 (TM7), Ala273 (TM7), Ile274 (TM7), Phe275 (TM7), Ser277 (TM7), **His278** (TM7), Asn280 (TM7)
3′-Me-CCPA	8	25	−11.9	Ala84 (TM3), Val87 (TM3), Leu88 (TM3), Leu90 (TM3), Thr91 (TM3), Gln92 (TM3), Met180 (TM5), Val181 (TM5), Asn184 (TM5), Val189 (TM5), Ser246 (TM6), Trp247 (TM6), Leu250 (TM6), His251 (TM6), **Asn254** (TM6), Ile270 (TM7), Ala273 (TM7), Ile274 (TM7), Phe275 (TM7), Ser277 (TM7), His278 (TM7), Asn280 (TM7)

[a] N_{tot} is the total number of clusters; the number of results in the top cluster is given by the frequency of occurrence, f_{occ}; ΔG_{bind} is the estimated free energy of binding for the top cluster results and is given in kcal/mol. The last column shows the contacting residues for the binding mode of the top cluster. Only residues with at least five van der Waals contacts to the ligand are shown. Residues that form hydrogen bonds with the ligand are highlighted in bold.

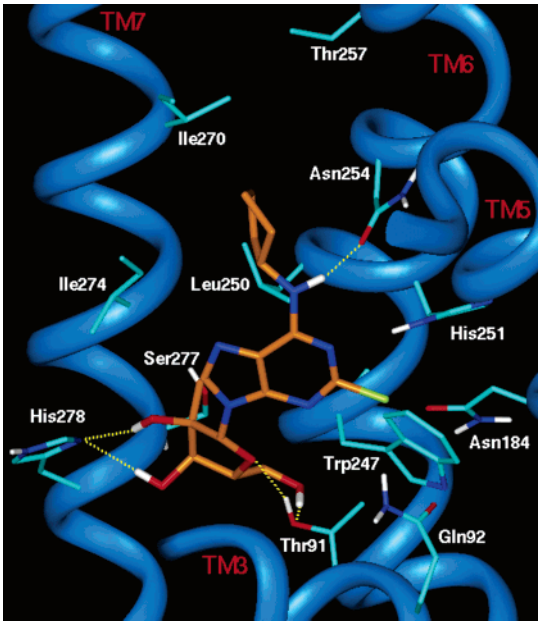

Figure 1. Side view of the 2′-Me-CCPA/bA$_1$AR complex model. The side chains of the important residues in proximity (5 Å) to the docked 2′-Me-CCPA molecule are highlighted and labeled.

oriented in a such a way that no hydrogen bond formation with the Asn254 side chain was possible.

To assess the dynamic stability of the 2′-Me-CCPA/bA$_1$AR and 3′-Me-CCPA/bA$_1$AR complexes and to analyze the potential ligand−receptor interactions, a molecular dynamics (MD) simulation of 150 ps at a constant temperature of 300 K was run. The distances between the ligands and the key receptor residues (Figure 2 of the Supporting Information) were monitored along the complete 150 ps MD trajectory. Examination of the average structure of the 2′-Me-CCPA/bA$_1$AR complex showed that the exocyclic amino group at the 6-position was located within hydrogen bonding distance from the CO oxygen of the Asn254 (TM6) side chain (Figure 1).

The trajectory plot of the analyzed complex (Figure 2a of the Supporting Information, on the left) shows that this hydrogen bond was quite stable throughout the MD simulation. Asn254, conserved among all adenosine receptor subtypes, was found to be important for ligand binding. In fact, the inability of the N250A mutant A$_3$AR[17] or the corresponding mutant A$_{2A}$AR[18] to bind either radiolabeled agonist or antagonist was consistent with a proposed direct interaction of this residue with our ligands. Moreover, from the MD trajectories (Figure 2b−e of the Supporting Information, on the left), it can be deduced that the ribose moiety of 2′-Me-CCPA/bA$_1$AR complex maintained a rather stable network of polar interactions during the MD simulation. After 50 ps of equilibration, in which the ligand merely underwent small amplitude fluctuations in the binding site, it rapidly achieved stable interactions with the receptor key residues throughout the rest of the trajectory. In particular, the 2′-OH, 3′-OH, and 5′-OH groups of the ribose ring were hydrogen-bonded to the N$^{\delta}$ imidazole nitrogen of His278 and the OH oxygen of Thr91, respectively, whereas the O-4′ oxygen interacted with the side chain oxygen of Thr91.

Surprisingly, 3′-Me-CCPA produced an instable complex with bA$_1$AR. In fact, with the exception of the hydrogen bond formed between the N^6 amino group of the ligand and the CO oxygen of Asn254 side chain, which remained stable along the 150 ps MD trajectory (Figure 2a of the Supporting Information, on the right), the remaining polar interactions resulted not strong enough to be preserved throughout the MD simulation, giving average distances longer than that of an ideal hydrogen bond (Figure 2b−e of the Supporting Information, on the right).

Figure 2 depicts a poor superimposition between the 2′-Me-CCPA and 3′-Me-CCPA inside the receptor binding domain. In particular, the adenine and the ribose moieties of the 3′-Me-CCPA derivative are shifted out of position with respect to those presented by the 2′-Me-CCPA analogue, decreasing the stability of the 3′-Me-CCPA/bA$_1$AR complex. A possible reason for these differences in the binding modes could be given by the fact that the ribose ring of 3′-Me-CCPA adopts a South (^{2}T$_3$)-syn conformation, in which the methyl group at position 3′ points toward the His278, thus preventing the hydrogen bonding formation of the OH groups at 2′ and 3′ positions with the N$^{\delta}$ imidazole nitrogen of His278. This fact might explain the different biological activity observed for the two examined compounds.

Our present model is consistent with several experimental results concerning recognition of the ribose or ribose-like moiety common to various adenosine agonists: (i) the hydrophilic interaction at His278 was required for high-affinity binding of both A$_1$ agonists and antagonists.[19] In the A$_{2A}$AR, this site was mutated to Ala with the loss of high-affinity binding of both agonists but not antagonists.[20] At the A$_3$AR, His at this site was proposed as the basis for enhanced affinity of

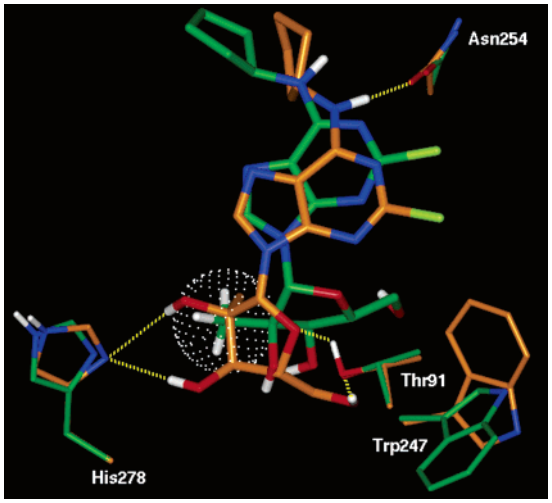

Figure 2. Superimposition of the docked structures of 2′-Me-CCPA (orange) and 3′-Me-CCPA (green). The van der Waals surface of the 3′-*C*-methyl of compound 3′-Me-CCPA, pointing toward His278 imidazole ring, is shown in white. The side chains of the important residues in proximity to the docked molecules are highlighted and labeled.

xanthine-7-ribosides relative to the parent xanthines.[21] (ii) Mutation of Thr91 to alanine in the A_1 and A_{2A} receptors, respectively, was shown to substantially decrease agonist affinity.[20,22]

As depicted in Figure 1, the cyclopentyl group of 2′-Me-CCPA appears to be surrounded by a hydrophobic pocket formed by Leu250 (TM6), Ile270 (TM7), Ile274 (TM7), and, to a lesser extent, by Thr257 (TM6), a pocket that contributes to an increase in the affinity and selectivity of 2′-*C*-methyl derivatives, in agreement with experimental data (see Table 1). Several items of mutational studies point toward these residues in the ligand-binding process. In fact, chimera and site-directed mutagenesis experiments identified Ile270 as being primarily responsible for species differences in the binding of N^6-adenine-substituted compounds.[23] The size of this hydrophobic pocket is large enough to accommodate bulkier N^6 substituents, such as the cyclohexyl group (compound **1**), determining an enhancement in A_1AR potency and a parallel gain in selectivity vs A_{2A} and A_3 ARs. In derivative **2**, the presence of the N^6-benzyl group, characterized by a higher degree of conformational flexibility, increases the steric hindrance inside the binding cavity, decreasing the relative stability of the complex. This may be the reason for the low A_1AR affinity of **2**. The chlorine atom of 2′-Me-CCPA favors the anchoring of the ligand into the binding site, making hydrophobic interactions with the Trp247 indole ring as well as slightly favorable electrostatic interactions with the Asn234 and Gln92 NH_2 groups (Figure 1). The interactions observed here could justify the enhanced potency of 2′-Me-CCPA (K_i = 3 nM) with respect to 2′-Me-CPA (K_i = 10 nM),[5] which does not have the chlorine atom at position 2. Mutation of Gln92 of the human A_{2A} adenosine receptor has been shown to affect agonist and antagonist binding.[22] Trp247, highly conserved in the G protein-coupled receptors (GPCRs) superfamily, has been postulated as playing a key role in the activation of GPCRs.[24] In fact, for hA_3AR, it has been found that the corresponding mutant W243A receptor is able to bind agonists but fails to activate the receptor.[17] In an UV absorption study,[25] it has been suggested that Trp265 in bovine rhodopsin (corresponding to Trp247 in bA_1AR) tilts toward the membrane plane during conversion of the inactive to the active state (MI → MII) of the receptor.

Conclusions

A series of 3′-*C*-methyl derivatives of N^6-substituted adenosine and 2-chloroadenosine, as well as of N^6-substituted adenosine-5′-*N*-uronamides were studied to determine their affinity toward bovine A_1, A_{2A}, and A_3 adenosine receptors. We found that the 3′-*C*-methyl modification in adenosine is not tolerated at all evaluated ARs subtypes. When this modification was combined with N^6-substitution with groups that induce high potency and selectivity at A_1AR such as the cyclopentyl one, the activity was in part restored and the selectivity increased. The 3′-*C*-methyl modification in adenosine-5′-*N*-uronamides was also not tolerated at all AR subtypes, even when this modification was combined with N^6-substitution with groups which induce high potency and selectivity at A_3AR, such as the 3-iodobenzyl one (3′-Me-IB-MECA).

In general it may be concluded that the introduction of a methyl group at *C*-3′ position in adenosine and adenosine derivatives is less tolerated than that in *C*-1′, or *C*-2′ or *C*-4′ positions of the ribose ring. This behavior might be explained by the marked preference of 3′-*C*-methyl analogues of adenosine to adopt in solution a South ($^2T_3$)-syn conformation around the glycosidic bond, which is not adequate for the binding at ARs. The 2′-*C*-methyl modification is better tolerated, in particular at A_1 receptor subtype. 2′-Me-CCPA was confirmed to be a potent and highly selective agonist at bovine A_1AR. Its potency and selectivity was maintained also at human A_1 AR. Thus, 2′-Me-CCPA proved to be the most selective agonist for human A_1 adenosine receptor versus human A_3 receptor so far known, and could be a useful pharmacological tool for investigation of A_1 adenosine receptor-mediated events.

Finally, a model of the bovine A_1AR was built to rationalize the higher affinity and selectivity of 2′-*C*-methyl derivatives of N^6-substituted-adenosine compared to that of 3′-*C*-methyl analogues. In the docking exploration, it was found that 2′-Me-CCPA was able to form a number of interactions with several polar residues in the transmembrane helices TM-3, TM-6, and TM-7 of bA_1AR which were not preserved in the molecular dynamics simulation of 3′-Me-CCPA/ bA_1AR complex.

Experimental Section

Chemistry. Melting points were determined on a Büchi apparatus and are uncorrected. Elemental analyses were determined on an EA 1108 CHNS-O (Fisons Instruments) analyzer. Thin-layer chromatography (TLC) was run on silica gel 60 F_{254} plates (Merck); silica gel 60 (70−230 mesh, Merck) for column chromatography was used. Nuclear magnetic resonance ^{1}H NMR spectra were determined with a Varian VXR-300 spectrometer at 300 MHz. The chemical shift values are expressed in δ values (parts per million) relative to tetramethylsilane as an internal standard. All exchangeable protons were confirmed by addition of D_2O. Stationary NOE experiments were run on degassed solutions at 25 °C. A presaturation delay of 1 s was used, during which the

decoupler low power was set at 20 dB attenuation. Mass spectroscopy was carried out on an HP 1100 series instrument. All measurements were performed in the positive ion mode using an atmospheric pressure electrospray ionization (API-ESI).

General Procedure for the Amination of 10, 12, and 13 into Compounds 1, 2, 4−6, 8. To a solution of **10**, **12**, or **13**[9] (1.0 mmol) in anhydrous EtOH (15 mL) under nitrogen atmosphere, the appropriate amine (molar ratio 1:6) was added. The reaction mixture was heated at reflux for the time reported below, concentrated in vacuo, and treated with methanolic ammonia (saturated at 0 °C) (30 mL) at room-temperature overnight to obtain the deblocked compounds which were purified by chromatography.

***N*⁶-Cyclohexyl-9*H*-(2-*C*-methyl-β-D-ribofuranosyl)adenine (1).** Reaction of **10** with cyclohexylamine for 2 h followed by chromatography on a silica gel column ($CHCl_3$−MeOH, 95:5) gave **1** as a white solid (82% yield). ^{1}H NMR (DMSO-d_6): δ 0.78 (s, 3H, CH_3), 1.35 (m, 4H, cyclohexyl), 1.60−1.90 (2m, 6H, cyclohexyl), 3.70, 3.80 (2m, 2H, H-5′), 3.90 (m, 1H, H-4′), 4.05 (m, 1H, C*H*NH), 4.10 (m, 1H, H-3′), 5.20 (m, 3H, OH), 5.95 (s, 1H, H-1′), 7.60 (d, J = 8.8 Hz, 1H, NH), 8.20 (s, 1H, H-2), 8.45 (s, 1H, H-8). MS: *m/z* 364.42 $[M + H]^+$. Anal. ($C_{17}H_{25}N_5O_4$) C, H, N.

***N*⁶-Benzyl-9*H*-(2-*C*-methyl-β-D-ribofuranosyl)adenine (2).** Reaction of **10** with benzylamine for 2 h followed by chromatography on a silica gel column ($CHCl_3$−MeOH, 94:6) gave **2** as a white solid (83% yield). ^{1}H NMR (DMSO-d_6): δ 0.80 (s, 3H, CH_3), 3.70 (m, 2H, H-5′), 3.80 (m, 1H, H-4′), 4.10 (dd, J = 6.8, 9.0 Hz, 1H, H-3′), 4.70 (br s, 2H, CH_2Ph), 5.20 (m, 3H, OH), 5.95 (s, 1H, H-1′), 7.30 (m, 5H, Ph), 8.20 (s, 1H, H-2), 8.40 (m, 1H, NH), 8.50 (s, 1H, H-8). MS: *m/z* 372.40 $[M + H]^+$. Anal. ($C_{18}H_{21}N_5O_4$) C, H, N.

***N*⁶-Cyclopentyl-9*H*-(3-*C*-methyl-β-D-ribofuranosyl)adenine (4).** Reaction of **12** with cyclopentylamine for 2 h followed by chromatography on a silica gel column ($CHCl_3$−MeOH, 97:3) gave **4** as a white solid (83% yield). ^{1}H NMR (DMSO-d_6): δ 1.30 (s, 3H, CH_3), 1.50−2.00 (2m, 8H, cyclopentyl), 3.60 (m, 2H, H-5′), 3.88 (br s, 1H, H-4′), 4.45 (t, J = 7.3 Hz, 1H, H-2′), 4.80 (s, 1H, OH), 5.40 (d, J = 7.0 Hz, 1H, OH), 5.80 (d, J = 7.7 Hz, 1H, H-1′), 5.93 (dd, J = 3.3, 8.4 Hz, 1H, OH), 7.82 (d, J = 7.0 Hz, 1H, NH), 8.15 (s, 1H, H-2), 8.32 (s, 1H, H-8). MS: *m*/z 350.39 $[M + H]^+$. Anal. ($C_{16}H_{23}N_5O_4$) C, H, N.

***N*⁶-Cyclohexyl-9*H*-(3-*C*-methyl-β-D-ribofuranosyl)adenine (5).** Reaction of **12** with cyclohexylamine for 3 h followed by chromatography on a silica gel column ($CHCl_3$−MeOH, 98:2) gave **5** as a white solid (89% yield). ^{1}H NMR (DMSO-d_6): δ 1.10−1.40 (m, 5H, cyclohexyl), 1.32 (s, 3H, CH_3), 1.60−1.96 (m, 5H, cyclohexyl), 3.60 (m, 2H, H-5′), 3.90 (t, J = 3.1 Hz, 1H, H-4′), 4.45 (t, J = 7.0 Hz, 1H, H-2′), 4.80 (s, 1H, OH), 5.40 (d, J = 5.9 Hz, 1H, OH), 5.82 (d, J = 8.1 Hz, 1H, H-1′), 5.90 (dd, J = 3.3, 8.4 Hz, 1H, OH), 7.70 (d, J = 8.4 Hz, 1H, NH), 8.15 (s, 1H, H-2), 8.35 (s, 1H, H-8), MS: *m/z* 364.42 $[M + H]^+$. Anal. ($C_{17}H_{25}N_5O_4$) C, H, N.

***N*⁶-Benzyl-9*H*-(3-*C*-methyl-β-D-ribofuranosyl)adenine (6).** Reaction of **12** with benzylamine for 2 h followed by chromatography on a silica gel column ($CHCl_3$−MeOH, 96:4) gave **6** as a white solid (79% yield). ^{1}H NMR (DMSO-d_6): δ 1.30 (s, 3H, CH_3), 3.60 (m, 2H, H-5′), 3.90 (br s, 1H, H-4′), 4.45 (t, J = 7.5 Hz, 1H, H-2′), 4.70 (m, 2H, CH_2Ph), 4.80 (s, 1H, OH), 5.4 (d, J = 7.0 Hz, 1H, OH), 5.80 (d and t, J = 8.1 Hz after exchange with D_2O, 2H, H-1′, OH), 7.30 (m, 5H, Ph), 8.18 (s, 1H, H-2), 8.35 (s, 1H, H-8), 8.50 (br s, 1H, NH). MS: *m/z* 372.40 $[M + H]^+$. Anal. ($C_{18}H_{21}N_5O_4$) C, H, N.

***N*⁶-Cyclopentyl-2-chloro-9*H*-(3-*C*-methyl-β-D-ribofuranosyl)adenine (8).** Reaction of **13** with cyclopentylamine for 3 h followed by chromatography on a silica gel column ($CHCl_3$−MeOH, 97:3) gave **8** as a white solid (68% yield). ^{1}H NMR (DMSO-d_6): δ 1.30 (s, 3H, CH_3), 1.50−2.00 (2m, 8H, cyclopentyl), 3.55 (m, 2H, H-5′), 3.85 (br s, 1H, H-4′), 4.40 (m, 2H, H-2′, C*H*NH), 4.87 (s, 1H, OH), 5.20 (t, J = 5.3 Hz, 1H, OH), 5.42 (d, J = 7.0 Hz, 1H, OH). 5.80 (d, J = 8.0 Hz, 1H, H-1′), 8.35 (s and d, 2H, NH, H-8). MS: *m/z* 384.84 $[M + H]^+$. Anal. ($C_{16}H_{22}ClN_5O_4$) C, H, N.

General Procedure for the Amination of 11, 12 and 13 into Compounds 3, 7 and 9. A stirred solution of **11**, **12** or **13** (1.0 mmol) in anhydrous EtOH (15 mL) was treated with 3-iodobenzylamine hydrochloride (1.1 mmol) and TEA (3.1 mmol), and the mixture was refluxed for the time reported below. The solvent was evaporated to dryness and the residue was dissolved in H_2O (20 mL) and extracted with CH_2Cl_2 (3 × 10 mL). The organic layers were dried over anhydrous Na_2SO_4, and evaporated to dryness. The oily residue was treated with methanolic ammonia (40 mL, saturated at 0 °C) and the solution was stirred at room-temperature overnight. After concentration in vacuo the residue was purified by chromatography.

***N*⁶-(3-Iodobenzyl)-2-chloro-9*H*-(2-*C*-methyl-β-D-ribofuranosyl)adenine (3).** Compound **3** was obtained starting from **11** (reaction time 2 h). Chromatography on a silica gel column ($CHCl_3$−MeOH, 96:4) gave **3** as a white solid (87% yield). ^{1}H NMR (DMSO-d_6): δ 0.80 (s, 1H, CH_3), 3.65−4.10 (m, 4H, H-3′, H-4′, H-5′), 4.60 (d, J = 5.5 Hz, 2H, CH_2Ph,), 5.20 (m, 2H, OH), 5.32 (s, 1H, OH), 5.85 (s, 1H, H-1′), 7.15 (t, J = 7.7 Hz, 1H, Ph), 7.35 (d, J = 7.7 Hz, 1H, Ph), 7.60 (d, J = 8.1 Hz, 1H, Ph), 7.75 (s, 1H, Ph), 8.55 (s, 1H, H-8), 8.90 (t, J = 5.5 Hz, 1H, NH). MS: *m/z* 532.74 $[M + H]^+$. Anal. ($C_{18}H_{19}ClIN_5O_4$) C, H, N.

***N*⁶-(3-Iodobenzyl)-9*H*-(3-*C*-methyl-β-D-ribofuranosyl)-adenine (7).** The title compound was obtained starting from **12** (reaction time 4 h). Chromatography on a silica gel column ($CHCl_3$−MeOH, 93:7) gave **7** as a white solid (80% yield). ^{1}H NMR (DMSO-d_6): δ 1.30 (s, 3H, CH_3), 3.60 (m, 2H, H-5′), 3.90 (br s, 1H, H-4′), 4.45 (t, J = 7.3 Hz, 1H, H-2′), 4.70 (br s, 2H, CH_2 Ph), 4.85 (s, 1H, OH), 5.40 (d, J = 6.6 Hz, 1H, OH), 5.85 (d and dd, J = 8.0 Hz after exchange with D_2O, 2H, H-1′, OH), 7.10 (t, J = 7.9 Hz, 1H, Ph), 7.35 (d, J = 7.7 Hz, 1H, Ph), 7.60 (d, J = 7.3 Hz, 1H, Ph), 7.70 (s, 1H, Ph), 8.20 (s, 1H, H-2), 8.40 (s, 1H, H-8), 8.55 (br s, 1H, NH). MS: *m/z* 498.29 $[M + H]^+$. Anal. ($C_{18}H_{20}IN_5O_4$) C, H, N.

***N*⁶-(3-Iodobenzyl)-2-chloro-9*H*-(3-*C*-methyl-β-D-ribofuranosyl)adenine (9).** Compound **9** was obtained starting from **13** (reaction time 4 h). Chromatography on a silica gel column ($CHCl_3$−MeOH, 96:4) gave **9** as a white solid (85% yield). ^{1}H NMR (DMSO-d_6): δ 1.30 (s, 3H, CH_3), 3.55 (m, 2H, H-5′), 3.90 (br s, 1H, H-4′), 4.35 (t, J = 7.3 Hz, 1H, H-2′), 4.60 (d, J = 5.5 Hz, 2H, CH_2Ph), 4.90 (s, 1H, OH), 5.17 (t, J = 5.3 Hz, 1H, OH), 5.43 (d, J = 7.0 Hz, 1H, OH), 5.80 (d, J = 8.1 Hz, 1H H-1′), 7.15 (t, J = 7.7 Hz, 1H, Ph), 7.30 (d, J = 7.0 Hz, 1H, Ph), 7.60 (d, J = 8.8 Hz, 1H, Ph), 7.74 (s, 1H, Ph), 8.45 (s, 1H, H-8), 9.00 (t, J = 6.0 Hz, 1H, NH). MS: *m/z* 532.74 $[M + H]^+$. Anal. ($C_{18}H_{19}ClIN_5O_4$) C, H, N.

6-Chloro-9*H*-(3-*C*-methyl-β-D-ribofuranosyl)purine (16). A mixture of **12** (1.0 g, 2.0 mmol) and methanolic ammonia (saturated at 0 °C, 50 mL) was stirred at room temperature for 4 h. Compound **16** precipitated from the reaction mixture, and the solid was filtered, washed with MeOH, and dried. The filtrate was evaporated to dryness, and the residue was purified by silica gel column chromatography ($CHCl_3$−MeOH 94:6) to give **16** as a white solid. Overall yield: 55%. ^{1}H NMR (DMSO-d_6): δ 1.30 (s, 3H, CH_3), 3.60 (m, 2H, H-5′), 3.90 (m, 1H, H-4′), 4.45 (t, J = 7.0 Hz, 1H, H-2′), 4.97 (s, 1H, OH), 5.20 (t, J = 4.9 Hz, 1H, OH), 5.50 (d, J = 6.6 Hz, 1H, OH), 6.04 (d, J = 7.7 Hz, 1H, H-1′), 8.82 (s, 1H, H-2), 8.95 (s, 1H, H-8). MS: *m/z* 301.70 $[M + H]^+$. Anal. ($C_{11}H_{13}ClN_4O_4$) C, H, N.

General Procedure for the Synthesis of 2′,3′-*O*-Isopropylidene Derivatives 17, 22, 29, and 32. A mixture of **3**, **7**, **16**, or **21** (1.0 mmol), 2,2-dimethoxypropane (18.1 mmol), camphorsulfonic acid (1.0 mmol) in anhydrous acetone (10 mL) was stirred at 55 °C for the time reported below. The solvent was removed in vacuo, and the residue was purified by chromatography.

6-Chloro-(3-*C*-methyl-2,3-*O*-isopropylidene-β-D-ribofuranosyl)purine (17). The title compound was obtained starting from **16** (reaction time 2 h). Chromatography on a silica gel column ($CHCl_3$−MeOH, 96:4) gave **17** as a white foam (72% yield). ^{1}H NMR (DMSO-d_6): δ 1.40 (s, 3H, CH_3), 1.53 (s, 6H, CH_3), 3.60 (m, 2H, H-5′), 4.12 (t, J = 5.8 Hz, 1H, H-4′),

4.95 (t, J = 4.9 Hz, 1H, OH), 5.03 (d, J = 1.8 Hz, 1H, H-2′), 6.24 (d, J = 2.2 Hz, 1H, H-1′), 8.82 (s, 1H, H-2) 8.87 (s, 1H, H-8). Anal. ($C_{14}H_{17}ClN_4O_4$) C, H, N.

9*H*-(3-*C*-Methyl-2,3-*O*-isopropylidene-β-D-ribofuranosyl)adenine (22). The title compound was obtained starting from **21** (reaction time 11 h). Chromatography on a silica gel column ($CHCl_3$−MeOH, 93:7) gave **22** as a white solid (58% yield). ^{1}H NMR (DMSO-d_6): δ 1.38 (s, 3H, CH_3), 1.53 (2s, 6H, CH_3), 3.60 (m, 2H, H-5′), 4.05 (m, 1H, H-4′), 4.96 (m, 2H, H-2′, OH), 6.08 (d, J = 2.2 Hz, 1H, H-1′), 7.35 (br s, 2H, NH_2), 8.15 (s, 1H, H-2), 8.32 (s, 1H, H-8). Anal. ($C_{14}H_{19}N_5O_4$) C, H, N.

***N*^{6}-(3-Iodobenzyl)-2-chloro-9*H*-(2-*C*-methyl-2,3-*O*-isopropylidene-β-D-ribofuranosyl)adenine (29)**. The title compound was obtained starting from **3** (reaction time 6 h). Chromatography on a silica gel column ($CHCl_3$−EtOAc, 99:1) gave **29** as a white solid (89% yield). ^{1}H NMR (DMSO-d_6): δ 1.15 (s, 3H, CH_3), 1.38 (s, 3H, CH_3), 1.55 (s, 3H, CH_3), 3.70 (m, 2H, H-5′), 4.25 (m, 1H, H-4′), 4.60 (m, 3H, H-3′, CH_2Ph), 5.26 (t, J = 5.5 Hz, 1H, OH), 6.15 (s, 1H, H-1′), 7.15 (t, J = 7.7 Hz, 1H, Ph), 7.35 (d, J = 8.1 Hz, 1H, Ph), 7.60 (d, J = 8.1 Hz, 1H, Ph) 7.75 (s, 1H, Ph), 8.40 (s, 1H, H-8), 8.95 (t, J = 6.0 Hz, 1H, NH). Anal. ($C_{21}H_{23}ClIN_5O_4$) C, H, N.

***N*^{6}-(3-Iodobenzyl)-2-chloro-9*H*-(3-*C*-methyl-2,3-*O*-isopropylidene-β-D-ribofuranosyl)adenine (32)**. The title compound was obtained starting from **7** (reaction time 4 h). Chromatography on a silica gel column ($CHCl_3$−MeOH, 99:1) gave **32** as a white solid (74% yield). ^{1}H NMR (DMSO-d_6): δ 1.30 (s, 3H, CH_3), 1.52 (2s, 6H, CH_3), 3.55 (m, 2H, OH), 4.10 (m, 1H, H-4′), 4.60 (d, J = 5.8 Hz, 2H, CH_2Ph), 4.90 (d, J = 2.6 Hz, 1H, H-2′), 6.0 (d, J = 2.6 Hz, 1H, H-1′), 7.15 (t, J = 7.7 Hz, 1H, Ph), 7.35 (d, J = 8.1 Hz, 1H, Ph), 7.60 (d, J = 8.1 Hz, 1H, Ph), 7.75 (s, 1H, Ph), 8.40 (s, 1H, H-8), 9.0 (pseudo t, 1H, NH). Anal. ($C_{21}H_{23}ClIN_5O_4$) C, H, N.

General Procedure for the Synthesis of Uronic Acids 18, 23, 30 and 33. A mixture of **17**, **22**, **29**, or **32** (1.0 mmol), BAIB (2.2 mmol), TEMPO (0.2 mmol) in 2 mL of 1:1 CH_3CN−H_2O solution was stirred at room temperature for the time reported below. A precipitate was obtained for compounds **23** and **33** which was filtered, triturated sequentially with diethyl ether and acetone, and dried in vacuo. In the case of compounds **18** and **30** the solvent was evaporated to dryness and the resulting residue was triturated with diethyl ether, filtered and dried in vacuo.

1-Deoxy-1-(6-chloro-9*H*-purin-9-yl)-3-*C*-methyl-2,3-*O*-isopropylidene-β-D-ribofuranoic acid (18). The title compound was obtained starting from **17** (reaction time 2 h) as a solid (80% yield). ^{1}H NMR (DMSO-d_6): δ 1.40 (s, 6H, CH_3), 1.52 (s, 3H, CH_3), 4.50 (s, 1H, CH_3), 4.78 (d, J = 1.8 Hz, 1H, H-2′), 6.38 (d, J = 1.8 Hz, 1H, H-1′), 8.57 (s, 1H, H-2), 8.80 (s, 1H, H-8), 13.0 (br s, 1H, COOH). Anal. ($C_{14}H_{15}ClN_4O_5$) C, H, N.

1-Deoxy-1-(6-amino-9*H*-purin-9-yl)-3-*C*-methyl-2,3-*O*-isopropylidene-β-D-ribofuranoic acid (23). Compound **23** was obtained starting from **22** (reaction time 3 h) as a solid (54% yield). ^{1}H NMR (DMSO-d_6): δ 1.38 (s, 3H, CH_3), 1.52, 1.56 (2s, 6H, CH_3), 4.60 (s, 1H, H-4′), 5.05 (d, J = 1.8 Hz, 1H, H-2′), 6.20 (d, J = 1.8 Hz, 1H, H-1′), 7.40 (br s, 2H, NH_2), 8.18 (s, 1H, H-2), 8.38 (s, 1H, H-8) 13.40 (br s, 1H, COOH). Anal. ($C_{14}H_{17}N_5O_5$) C, H, N.

1-Deoxy-1-[*N*^{6}-(3-iodobenzyl)-2-chloro-9*H*-purin-9-yl]-2-*C*-methyl-2,3-*O*-isopropylidene-β-D-ribofuranoic acid (30). The title compound was obtained starting from **29** (reaction time 3 h), as a solid (90% yield). ^{1}H NMR (DMSO-d_6): δ 1.08 (s, 3H, CH_3), 1.40 (s, 3H, CH_3), 1.52 (s, 3H, CH_3), 4.57 (d, J = 1.9 Hz, 2H, CH_2Ph), 4.77 (s, 1H, H-4′), 5.03 (s, 1H, H-3′), 6.28 (s, 1H, H-1′), 7.15 (q, J = 7.9 Hz, 1H, Ph), 7.36 (d, J = 7.0 Hz, 1H, Ph), 7.60 (d, J = 7.6 Hz, 1H, Ph), 7.76 (s, 1H, Ph), 8.50 (s, 1H, H-8), 8.96 (t, J = 6.0 Hz, 1H, NH), 13.30 (br s, 1H, COOH). Anal. ($C_{21}H_{21}ClIN_5O_5$) C, H, N.

1-Deoxy-1-[*N*^{6}-(3-iodobenzyl)-2-chloro-9*H*-purin-9-yl]-3-*C*-methyl-2,3-*O*-isopropylidene-β-D-ribofuranoic acid (33). The title compound was obtained starting from **32** (reaction time 2 h), as a solid (74% yield). ^{1}H NMR (DMSO-d_6): δ 1.30 (s, 1H, CH_3), 1.46 (s, 3H, CH_3), 1.48 (s, 3H, CH_3), 4.60 (br s, 3H, CH_2Ph, H-4′), 5.02 (s, 1H, H-2′), 6.20 (s, 1H, H-1′), 7.15 (t, J = 7.7 Hz, 1H, Ph), 7.38 (d, J = 7.3 Hz, 1H, Ph) 7.60 (d, J = 7.7 Hz, 1H, Ph), 7.72 (s, 1H, Ph), 8.42 (s, 1H, H-8), 9.0 (br s, 1H, NH), 13.30 (br s, 1H, COOH). Anal. ($C_{21}H_{21}ClIN_5O_5$) C, H, N.

General Procedure for the Synthesis of Ethyl Esters 19, 24, 31, and 34. To a solution of **18**, **23**, **30**, or **33** (0.65 mmol) in anhydrous EtOH (28 mL) at 0 °C was added dropwise 0.23 mL of $SOCl_2$ and the solution was stirred under nitrogen atmosphere at room temperature for the time reported below. After evaporation in vacuo the residue was purified by chromatography.

Ethyl 1-Deoxy-1-(6-chloro-9*H*-purin-9-yl)-3-*C*-methyl-2,3-*O*-isopropylidene-β-D-ribofuranuroate (19). The title compound was obtained starting from **18** (reaction time 3 h). Chromatography on a silica gel column ($CHCl_3$−MeOH, 99:1) gave **19** as a foam containing a small amount of the inseparable ethyl 1-deoxy-1-(6-ethoxy-9*H*-purin-9-yl)-3-*C*-methyl-2,3-*O*-isopropylidene-β-D-ribofuranuroate (overall yield 48%).

Ethyl 1-Deoxy-1-(6-amino-9*H*-purin-9-yl)-3-*C*-methyl-2,3-*O*-isopropylidene-β-D-ribofuranuroate (24). The title compound was obtained starting from **23** (reaction time 7 h). Chromatography on a silica gel column ($CHCl_3$−MeOH, 92:8) gave **24** as a white solid (62% yield). ^{1}H NMR (DMSO-d_6): δ 1.20 (t, J = 7.0 Hz, 3H, CH_3CH$_2$), 1.40 (s, 3H, CH_3), 1.50 (s, 3H, CH_3), 1.53 (s, 3H, CH_3), 4.15 (pseudo t, 2H, CH_2CH$_3$), 4.70 (s, 1H, H-4′), 5.15 (s, 1H, H-2′), 6.25 (s, 1H, H-1′), 7.40 (br s, 2H, NH_2), 8.18 (s, 1H, H-2), 8.38 (s, 1H, H-8). Anal. ($C_{16}H_{21}N_5O_5$) C, H, N.

Ethyl 1-Deoxy-1-[*N*^{6}-(3-iodobenzyl)-2-chloro-9*H*-purin-9-yl]-2-*C*-methyl-2,3-*O*-isopropylidene-β-D-ribofuranuroate (31). The title compound was obtained starting from **30** (reaction time 7 h). Chromatography on a silica gel column ($CHCl_3$−EtOAc, 95:5) gave **31** as a white solid (57% yield). ^{1}H NMR (DMSO-d_6): δ 1.06 (t, J = 7.1 Hz, 3H, CH_3CH$_2$), 1.18 (s, 3H, CH_3), 1.44 (s, 3H, CH_3), 1.52 (s, 3H, CH_3), 4.0 (m, 2H, CH_2CH$_3$), 4.60 (d, J = 6.2 Hz, 2H, CH_2Ph), 4.82 (d, J = 2.9 Hz, 1H, H-4′), 5.25 (d, J = 2.6 Hz, 1H, H-3′), 6.30 (s 1H, H-1′), 7.15 (t, J = 7.7 Hz, 1H, Ph), 7.35 (d, J = 8.1 Hz, 1H, Ph), 7.60 (d, J = 8.1 Hz, 1H, Ph), 7.75 (s, 1H, Ph), 8.37 (s, 1H, H-8), 9.0 (t, J = 6.0 Hz, 1H, NH). Anal. ($C_{23}H_{25}ClIN_5O_5$) C, H, N.

Ethyl 1-Deoxy-1-[*N*^{6}-(3-iodobenzyl)-2-chloro-9*H*-purin-9-yl]-3-*C*-methyl-2,3-*O*-isopropylidene-β-D-ribofuranuroate (34). The title compound was obtained starting from **33** (reaction time 6 h at 40 °C). Chromatography on a silica gel column ($CHCl_3$−EtOAc, 95:5) gave **34** as a white solid (60% yield). ^{1}H NMR (DMSO-d_6): δ 1.12 (t, J = 7.1 Hz, 3H, CH$_2$CH_3), 1.40 (s, 3H, CH_3), 1.55 (2s, 6H, CH_3), 4.10 (m, 2H, CH_2CH$_3$), 4.60 (d, J = 5.9 Hz, 2H, CH_2Ph), 4.70 (s, 1H, H-4′), 5.10 (d, J = 1.5 Hz, 1H, H-2′), 6.20 (d, J = 1.5 Hz, 1H, H-1′), 7.12 (t, J = 7.7 Hz, 1H, Ph), 7.35 (d, J = 7.7 Hz, 1H, Ph), 7.60 (d, J = 8.0 Hz, 1H, Ph), 7.73 (s, 1H, Ph), 8.40 (s, 1H, H-8), 9.0 (t, J = 6.0 Hz, 1H, NH). Anal. ($C_{23}H_{25}ClIN_5O_5$) C, H, N.

Ethyl 1-Deoxy-1-[*N*^{6}-(3-iodobenzyl)-9*H*-purin-9-yl]-3-*C*-methyl-2,3-*O*-isopropylidene-β-D-ribofuranuroate (20). A stirred solution of **19** (1.0 mmol) in anhydrous EtOH (15 mL) was treated with 3-iodobenzylamine hydrochloride (1.1 mmol) and TEA (3.1 mmol), and the mixture was refluxed for 6 h. The solvent was evaporated to dryness, and the residue was dissolved in H_2O (20 mL) and extracted with CH_2Cl_2 (3 × 10 mL). The organic layers were dried over anhydrous Na_2SO_4 and concentrated under reduced pressure. The oily residue was purified by chromatography on a silica gel column ($CHCl_3$−EtOAc, 96:4) to give **20** as a white solid (60% yield). ^{1}H NMR (DMSO-d_6): δ 1.15 (t, J = 7.1 Hz, 3H, CH$_2$CH_3), 1.37 (s, 3H, CH_3), 1.50 (s, 3H, CH_3), 1.55 (s, 3H, CH_3) 4.15 (m, 2H, CH_2CH$_3$), 4.65 (br s, 2H, CH_2Ph), 4.72 (s, 1H, H-4′), 5.15 (d, J = 1.8 Hz, 1H, H-2′), 6.25 (d, J = 1.8 Hz, 1H, H-1′), 7.10 (t, J = 7.9 Hz, 1H, Ph), 7.35 (d, J = 7.3 Hz, 1H, Ph), 7.56 (d, J = 7.3 Hz, 1H, Ph), 7.75 (s, 1H, Ph), 8.22 (s, 1H, H-2), 8.40 (s, 1H, H-8), 8.53 (br s, 1H, NH). Anal. ($C_{23}H_{26}IN_5O_5$) C, H, N.

General Procedure for the Synthesis of Uronamides 14, 15, 25, and 26. A mixture of **20**, **24**, **31**, or **34** (0.14 mmol) and the suitable amine (1.1 mL) was stirred at −20 °C for 3 h

and then at room-temperature overnight. The solution was evaporated to dryness, and then 90% HCOOH was added and stirred at 45 °C for 7 h. The solvent was removed in vacuo, and the residue was coevaporated with MeOH (4 × 10 mL), and then purified by chromatography.

***N*-Ethyl-1-deoxy-1-(6-amino-9*H*-purin-9-yl)-3-*C*-methyl-β-D-ribofuranuronamide (14)**. The title compound was obtained starting from **24** and anhydrous ethylamine. Chromatography on a silica gel column ($CHCl_3$−MeOH, 85:15) gave **14** as a white solid (60% yield). ^{1}H NMR (DMSO-d_6): δ 1.10 (t, J = 7.3 Hz, 3H, CH_3CH$_2$), 1.18 (s, 3H, CH$_3$), 3.20 (m, 2H, CH_2CH$_3$), 4.22 (s, 1H, H-4′), 4.40 (t, J = 7.0 Hz, 1H, H-2′), 5.30 (s, 1H, OH), 5.60 (d, J = 7.0 Hz, 1H, OH), 5.90 (d, J = 8.1 Hz, 1H, H-1′), 7.45 (br s, 2H, NH$_2$), 8.20 (s, 1H, H-2), 8.45 (s, 1H, H-8), 9.18 (t, J = 5.5 Hz, 1H, NH). MS: *m/z* 323.33 [M + H]$^+$. Anal. ($C_{13}H_{18}N_6O_4$) C, H, N.

***N*-Methyl-1-deoxy-1-[*N*^{6}-(3-iodobenzyl)-9*H*-purin-9-yl]-3-*C*-methyl-β-D-ribofuranuronamide (15)**. The title compound was obtained starting from **20** and anhydrous methylamine. Chromatography on a silica gel column ($CHCl_3$−MeOH, 94:6) gave **15** as a white solid (66% yield). ^{1}H NMR (DMSO-d_6): δ 1.15 (s, 3H, CH$_3$), 2.70 (d, J = 4.0 Hz, 3H, CH_3NH), 4.23 (s, 1H, H-4′), 4.40 (m, 1H, H-2′), 4.68 (m, 2H, CH_2Ph), 5.32 (s, 1H, OH), 5.60 (d, J = 6.8 Hz, 1H, OH), 5.94 (d, J = 8.1 Hz, 1H, H-1′), 7.10 (t, J = 7.5 Hz, 1H, Ph), 7.35 (d, J = 7.0 Hz, 1H, Ph), 7.58 (d, J = 8.8 Hz, 1H, Ph), 7.72 (s, 1H, Ph), 8.32 (s, 1H, H-2), 8.52 (s, 1H, H-8), 8.60 (br s, 1H, N*H*CH$_3$), 9.14 (s, 1H, NH). MS: *m/z* 525.32 [M + H]$^+$. Anal. ($C_{19}H_{21}IN_6O_4$) C, H, N.

***N*-Methyl-1-deoxy-1-[(*N*^{6}-3-iodobenzyl)-2-chloro-9*H*-purin-9-yl]-2-*C*-methyl-β-D-ribofuranuronamide (25)**. The title compound was obtained starting from **31**. Chromatography on a silica gel column ($CHCl_3$−MeOH, 97:3) gave **25** as a white solid (70% yield). ^{1}H NMR (DMSO-d_6): δ 0.80 (s, 3H, CH$_3$), 2.70 (d, J = 4.4 Hz, 3H, CH_3NH), 4.0 (pseudo t, 1H, H-3′), 4.26 (d, J = 8.1 Hz, 1H, H-4′), 4.55 (d, J = 5.5 Hz, 2H, CH_2Ph), 5.46 (s, 1H, OH), 5.60 (d, J = 5.5 Hz, 1H, OH), 5.88 (s, 1H, H-1′), 7.10 (t, J = 7.7 Hz, 1H, Ph), 7.32 (d, J = 8.1 Hz, 1H, Ph), 7.58 (d, J = 7.3 Hz, 1H, Ph), 7.70 (s, 1H, Ph), 8.40 (br s, 1H, N*H*CH$_3$), 8.98 (pseudo t, 1H, N*H*CH$_2$). MS: *m/z* 559.76 [M + H]$^+$. Anal. ($C_{19}H_{20}ClIN_6O_4$) C, H, N.

***N*-Methyl-1-deoxy-1-[*N*^{6}-(3-iodobenzyl)-2-chloro-9*H*-purin-9-yl]-3-*C*-methyl-β-D-ribofuranuronamide (26)**. The title compound was obtained starting from **34**. Chromatography on a silica gel column ($CHCl_3$−MeOH, 97:3) gave **26** as a white solid (86% yield). ^{1}H NMR (DMSO-d_6): δ 1.12 (s, 3H, CH$_3$), 2.70 (d, J = 4.6 Hz, 3H, CH_3NH), 4.22 (s, 1H, H-4′), 4.30 (d, J = 6.7 Hz, 1H, H-2′), 4.60 (d, J = 5.5 Hz, 2H, CH_2Ph), 5.35 (s, 1H, OH), 5.60 (d, J = 6.1 Hz, 1H, OH), 5.85 (d, J = 8.2 Hz, 1H, H-1′), 7.10 (t, J = 7.8 Hz, 1H, Ph), 7.34 (d, J = 7.9 Hz, 1H, Ph), 7.58 (d, J = 7.9 Hz, 1H, Ph), 7.72 (s, 1H, Ph), 8.48 (d, J = 4.3 Hz, 1H, N*H*CO), 8.58 (s, 1H, H-8), 9.05 (t, J = 5.7 Hz, 1H, N*H*CH$_2$). MS: *m/z* 559.76 [M + H]$^+$. Anal. ($C_{19}H_{20}ClIN_6O_4$) C, H, N.

***N*-Methyl-1-deoxy-1-[(*N*^{6}-3-iodobenzyl)-2-methylamine-9*H*-purin-9-yl]-2-*C*-methyl-β-D-ribofuranuronamide (27)**. A mixture of **25** (90 mg, 0.16 mmol) and 2 N CH_3NH_2/THF (13.4 mL) was heated in Parr bomb for 20 h at 70 °C. The solution was evaporated to dryness, and the residue was purified by chromatography on a silica gel column ($CHCl_3$−MeOH, 93:7) to obtain **27** as a white solid (45% yield). ^{1}H NMR (DMSO-d_6): δ 0.85 (s, 3H, CH$_3$), 2.65 (d, J = 4.8 Hz, 3H, NHCH_3), 2.75 (d, J = 4.8 Hz, NHCH_3), 4.25 (m, 2H, H-4′, H-3′), 4.58 (br s, 2H, CH_2Ph), 5.25 (s, 1H, OH), 5.54 (d, J = 5.8 Hz, 1H, OH), 5.81 (s, 1H, H-1′), 6.33 (d, J = 5.4 Hz, 1H, N*H*CH$_3$), 7.10 (t, J = 7.7 Hz, 1H, Ph), 7.40 (d, J = 8.0 Hz, Ph), 7.56 (d, J = 8.0 Hz, 1H, Ph), 7.75 (s, 1H, Ph), 7.97 (br s, 1H, CH$_3$N*H*CO), 8.25 (s, 1H, N*H*CH$_2$), 8.30 (s, 1H, H-8). MS: *m/z* 554.36 [M + H]$^+$. Anal. ($C_{20}H_{24}IN_7O_4$) C, H, N.

***N*-Methyl-1-deoxy-1-[*N*^{6}-(3-iodobenzyl)-2-methylamine-9*H*-purin-9-yl]-3-*C*-methyl-β-D-ribofuranuronamide (28).** Compound **28** was obtained starting from **26** (90 mg, 0.16 mmol) as described for **27** (reaction time 3 days at 90 °C). Chromatography on a silica gel column ($CHCl_3$−MeOH, 93:7) gave **28** as a white solid (51% yield). ^{1}H NMR (DMSO-d_6): δ 1.15 (s, 3H, CH$_3$), 2.68 (d, J = 4.4 Hz, 3H, NHCH_3), 2.77 (d, J = 4.4 Hz, 3H, NHCH_3), 4.20 (s, 1H, H-4′), 4.60 (br s, 3H, CH_2Ph, H-2′), 5.22 (s, 1H, OH), 5.55 (d, J = 6.1 Hz, 1H, OH), 5.82 (d, J = 8.0 Hz, 1H, H-1′), 6.28 (d, J = 4.4 Hz, 1H, N*H*CH$_3$), 7.10 (t, J = 7.7 Hz, 1H, Ph), 7.38 (d, J = 7.7 Hz, 1H, Ph), 7.58 (d, J = 7.3 Hz, 1H, Ph), 7.76 (s, 1H, Ph), 8.10 (br s, 1H, CH$_3$N*H*CO), 8.15 (s, 1H, H-8), 8.35 (br s, 1H, N*H*CH$_2$). MS: *m/z* 554.36 [M + H]$^+$. Anal. ($C_{20}H_{24}IN_7O_4$) C, H, N.

Computational Procedures. All model building, energy minimizations, and molecular dynamics calculations were carried out using SYBYL 6.9[26] and AMBER 4.1[27,28] modeling packages, respectively. All manipulations were performed on a Silicon Graphics R12000 workstation.

Adenosine A_1 Receptor Model Building. The structural model of the human A_1AR was built using the recently reported 2.8 Å crystal structure of bovine rhodopsin[15] (PDB entry code: 1F88) as a structural template. Briefly, sequences of the human A_1AR transmembrane domains were amended by comparison to the corresponding domains of rhodopsin, according to a published sequence alignment.[29] Individual TM helical segments were built as ideal helices (using $\phi-\psi$ angles of −63.0° and −41.6°) with side chains placed in prevalent rotamers and representative proline kink geometries. Each model helix was capped with an acetyl group at the N-terminus and an *N*-methyl group at the C-terminus. These structures were then grouped by adding one at a time until a helical bundle (TM region), matching the overall characteristics of the crystallographic structure of rhodopsin, had been obtained. The relative orientations and interactions between the helices were adjusted based on incorporated structural inferences from available experimental data, such as mutation and ligand binding studies,[30] cysteine scanning data,[31] and site-directed mutation experiments.[32] Because earlier work showed that polarity conserved positions cluster together in the cores of proteins to create conserved hydrogen-bonding interactions,[33] we refined the model by applying the additional hydrogen-bonding constraints between the conserved polar residues Asn27, Asp55, and Asn284 in accordance with data from site-directed mutagenesis.[32,33] The helical bundle was subjected to energy-minimization using the SANDER module of the AMBER suite of programs[27,28] until the rms value of the coniugate gradient was 0.001 kcal/mol per Å. An energy penalty force constant of 5 kcal/Å^2/mol on the protein backbone atoms was applied throughout these calculations.

For the conformational refinement of the bA_1AR, the minimized structure was then used as the starting point for subsequent 200 ps of molecular dynamics (MD), during which the positional constraints on the protein backbone atoms were gradually released from 5 to 0.05 kcal/Å^2/mol. The options of MD at 300 K with 0.2 ps coupling constant were a time step of 1 fs and a nonbonded update every 25 fs. The lengths of bonds with hydrogen atoms were constrained according to the SHAKE algorithm.[34] The average structure from the last 50 ps trajectory of MD was reminimized with backbone constraints in the secondary structure. The conformational validity of main chain and side chain torsions in each residue within the protein models was analyzed using the PROCHECK program.[35] Also, all ω angles for the peptide planarity were measured. The chirality of all Cα atoms, which in naturally occurring amino acids is of the l-configuration, was checked. RMS deviations between backbone atoms in all helices were compared to the X-ray structure of rhodopsin as a template.

Docking Simulations. Docking was performed with version 3.05 of the program AutoDock.[16] It combines a rapid energy evaluation through precalculated grids of affinity potentials with a variety of search algorithms to find suitable binding positions for a ligand on a given protein. While the protein is required to be rigid, the program allows torsional flexibility in the ligand. Docking to bA_1AR was carried out using the empirical free energy function and the Lamarckian genetic algorithm, applying a standard protocol, with an initial population of 50 randomly placed individuals, a maximum number of 1.5 × 10^6 energy evaluations, a mutation rate of

0.02, a crossover rate of 0.80, and an elitism value of 1. Proportional selection was used, where the average of the worst energy was calculated over a window of the previous 10 generations. For the local search, the so-called pseudo-Solis and Wets algorithm was applied using a maximum of 300 iterations per local search. The probability of performing local search on an individual in the population was 0.06, and the maximum number of consecutive successes or failures before doubling or halving the local search step size was 4.50 independent docking runs were carried out for each ligand. Results differing by less than 1.5 Å in positional root mean-square deviation (rmsd) were clustered together and represented by the result with the most favorable free energy of binding.

(1) Ligand Setup. The core structures of 2′-Me-CCPA and 3′-Me-CCPA were retrieved from the Cambridge Structural Database (CSD)[36] and modified using standard bond lengths and bond angles of the SYBYL fragment library. The CSD refcodes of the ligands are GIDZIC and BOSGEV, respectively. Geometry optimizations were realized with the SYBYL/Maximin2 minimizer by applying the BFGS (Broyden, Fletcher, Goldfarb, and Shannon) algorithm[37] and setting a rms gradient of the forces acting on each atom of 0.05 kcal/mol Å as the convergence criterion. Atomic charges were assigned using the Gasteiger−Marsili formalism,[38] which is the type of atomic charges used in calibrating the AutoDock empirical free energy function. Finally, the two compounds were setup for docking with the help of AutoTors, the main purpose of which is to define the torsional degrees of freedom to be considered during the docking process. The number of flexible torsions defined for each ligand is five.

Superimposition of the geometry-optimized ligand structures was carried out using the "Fit Atoms" method implemented in SYBYL. The quality of the fit is represented by the rms value computed for the matched atoms.

(2) Protein Setup. The energy-minimized structure of bA$_1$AR model was setup for docking as follows: polar hydrogens were added using the biopolymers module of the SYBYL program, (Arg, Lys, Glu, and Asp residues were considered ionized while all His were considered neutral by default), and Kollman united-atom partial charges were assigned. Solvation parameters were added to the final protein file using the Addsol utility of AutoDock. The grid maps representing the proteins in the actual docking process were calculated with AutoGrid. The grids (one for each atom type in the ligand, plus one for electrostatic interactions) were chosen to be sufficiently large to include not only the active site but also significant portions of the surrounding surface. The dimensions of the grids were thus 50 Å × 40 Å × 40 Å, with a spacing of 0.375 Å between the grid points.

Molecular Dynamics Simulations. Refinement of the ligand/receptor bound complex was achieved by in vacuo energy minimization with the SANDER module of AMBER 4.1 (50 000 steps; distance dependent dielectric function of $\epsilon = 4r$), applying an energy penalty force constant of 5 kcal/mol on the protein backbone atoms. The geometry-optimized complexes were then used as the starting point for subsequent 150 ps MD simulation, during which the protein backbone atoms were constrained as done in the previous step. The simulations employed the Cornell force field,[39] as implemented in the AMBER 4.1 suite of programs. The additional parameters required for the ligands were derived by analogy to existing parameters. Partial atomic charges for the ligands were imported from the output files of AM1 full geometry optimizations as implemented in the MOPAC 6.0 program.[40] A time step of 1 fs and a nonbonded pairlist updated every 25 fs were used for the MD simulations. The temperature was mantained at 300 K using the Berendsen algorithm73 with a 0.2 ps coupling constant. An average structure was calculated from the last 100 ps trajectory and energy-minimized using the steepest descent and conjugate gradient methods as specified above. The MD trajectories were analyzed by means of the CARNAL module of AMBER package.

Biological Methods. Materials. [^{3}H]1,3-dipropyl-8-cyclopentylxanthine ([^{3}H]DPCPX) (specific activity 108 Ci/mmol), [^{3}H](2-[4-(2-carboxyethyl)phenyl]ethyl-amino-5′-*N*-ethylcarboxyamido-adenosine ([^{3}H]CGS21680) specific activity 42.5 Ci/mmol), [^{125}I]N^6-(3-iodo-4-aminobenzyl)-5′-*N*-methylcarboxamidoadenosine ([^{125}I]AB-MECA) (specific activity 2000 Ci/mmol), and [α-^{32}P]ATP were purchased from PerkinElmer Life Sciences. CHA and DPCPX were purchased from Research Biochemical Incorporated (RBI, Natick, MA). Adenosine deaminase, forskolin, and GTP were from Sigma-Aldrich. Myokinase and creatine kinase were purchased from Boehringer-Mannheim (Mannheim, Germany). All other reagents were from standard commercial sources and of the highest grade commercially available.

Receptor Binding Assay and Adenylyl Cyclase Assay. Displacement of [^{3}H]DPCPX from A$_1$ adenosine receptor in bovine cortical membranes was performed as described;[13] displacement of [^{3}H]CGS-21680 from A$_{2A}$AR in bovine striatal membranes and [^{125}I]AB-MECA from A$_3$AR in bovine cortical membranes were performed as described elsewhere.[14] Compounds were dissolved in DMSO and diluted with assay buffer to the final concentration where the amount of DMSO never exceeded 2%. At least six different concentration of each compound were used. The experiments ($n = 4$), carried out in triplicate, were analyzed by an iterative curve fitting procedure (GraphPad, Prism program, San Diego, CA), which provided IC$_{50}$ and SEM values for tested compounds. IC$_{50}$ values were converted to K_i values using the Cheng and Prusoff equation.[41] The dissociation constant (K_d) of [^{3}H]DPCPX, [^{3}H]CGS-21680, and [^{125}I]AB-MECA was 0.5, 14, and 1.02 nM, respectively. Adenylyl cyclase assay was performed as previously described.[5]

Binding Assay and Adenylyl Cyclase Assay at Cloned Human Adenosine Receptors. K_i values were determined in competition experiments with membranes from CHO cells stably transfected with the individual human adenosine receptor subtypes.[42] For A$_1$ receptors, 1 nM [^{3}H]CCPA was used as a radioligand, and [^{3}H]NECA was used for the A$_{2A}$ (30 nM) and A$_3$ subtypes (10 nM). The relative potency (EC$_{50}$ values) at A$_{2B}$ adenosine receptors was determined measuring the activation of adenylyl cyclase in a membrane preparation of CHO cells stably transfected with the human A$_{2B}$ subtype following the procedure described earlier.[42]

Acknowledgment. This project was supported by a grant from University of Camerino and by the Italian MIUR funds (PRIN 2002). The work was presented in part at the 2003 meeting "Purinergic Receptors-Medicinal Chemistry and Pharmacology of Purinergic Receptors" (Camerino, Italy). We thank M. Brandi, F. Lupidi, G. Rafaiani, and M. Ricciutelli for technical assistance.

Supporting Information Available: Dose−response curves for the inhibition of forskolin-stimulated adenylyl cyclase in rat cortical membranes induced by compounds **3**, **4**, **8**, **25** and **26** (Figure 1), plots of the monitored distance between the key residues of 2′-Me-CCPA and 3′-Me-CCPA and the amino acids Asn254, His278 and Thr91 along the complete MD trajectory (Figure 2), and elemental analytical data for all new compounds. This material is available free of charge via the Internet at http://pubs.acs.org.

References

(1) Fredholm, B. B.; IJzerman, A. P.; Jacobson, K. A.; Klotz, K.-N.; Linden, J. International Union of Pharmacology. XXV. Nomenclature and classification of adenosine receptors. *Pharmacol. Rev.* **2001**, *53*, 527−552.
(2) Fredholm, B. B. Adenosine receptors as targets for drug development. *Drug News Perspect.* **2003**, *16*, 283−289.
(3) Saloranta, C.; Franssila, K.; Ekstrand, A.; Taskinen, M. R.; Groop, L. Modulation of hepatic glucose production by non-esterified fatty acids in type 2 (noninsulin-dependent) diabetes mellitus. *Diabetologia* **1991**, *34*, 409−415.

(4) Beukers, M. W.: Chang, L. C.; von Frijtag Drabbe Kunzel, J. K.; Mulder-Krieger, T.; Spanjersberg, R. F.; Brussee, J.; IJzerman, A. P. New, nonadenosine, high-potency agonists for the human adenosine A2B receptor with an improved selectivity profile compared to the reference agonist *N*-ethylcarboxamidoadenosine. *J. Med. Chem.* **2004**, *47*, 3707−3709.
(5) Franchetti, P.; Cappellacci, L.; Marchetti, S.; Trincavelli, L.; Martini, C.; Mazzoni, M. R.; Lucacchini, A.; Grifantini, M. 2′-*C*-Methyl analogues of selective adenosine receptor agonists: synthesis and binding studies. *J. Med. Chem.* **1998**, *41*, 1708−1715.
(6) Cappellacci, L.; Barboni, G.;Palmieri, M.; Pasqualini, M.; Grifantini, M.; Costa, B.; Martini, C.; Franchetti, P. Ribose-modified nucleosides as ligands for adenosine receptors: synthesis, conformational analysis and biological evaluation of 1′-*C*-methyl adenosine analogues. *J. Med. Chem.* **2002***, 45,* 1196−1202.
(7) Lohse, M. J.; Klotz, K.-N., Schwabe, U.; Cristalli, G.; Vittori, S.; Grifantini, M. 2-Chloro-N^6-cyclopentyladenosine: a highly selective agonist at A_1 adenosine receptors. *Naunyn Schmiedeberg's Arch. Pharmacol.* **1988**, *337*, 687−689.
(8) (a) Ralevic, V.; Burnstock, G. Receptors for purines and pyrimidines. *Pharmacol. Rev.* **1998**, *50*, 413−492. (b) Kim, H. O.; Ji, X.-D.; Siddiqi, S. M.; Olah, M. E.; Stiles, G. L.; Jacobson, K. A. 2-Substitution of *N*^{6}-benzyladenosine-5′-uronamides enhances selectivity for A_3 adenosine receptors. *J. Med. Chem.* **1994**, *37*, 3614−3621.
(9) Franchetti, P.; Cappellacci, L,; Pasqualini, M.; Petrelli, R.; Vita, P.; Jayaram, H. N.; Horvath, Z.; Szekeres, T.; Grifantini, M. Manuscript in preparation.
(10) Epp, J. B. and Widlanski, T. S. Facile preparation of nucleoside-5′-carboxylic acids. *J. Org. Chem.* **1999**, *64*, 293−295.
(11) Nutt, R. F.; Dickinson, M. J.; Holly, F. W.; Walton, E. Branched-chain sugar nucleosides. III. 3′-*C*-Methyladenosine. *J. Org. Chem.* **1968**, *33*, 1789−1795.
(12) Rosemeyer, H.; Toth, G.; Golankiewicz, B.; Kazimierczuk, Z.; Bourgeois, W.; Kretschmer, U.; Muth, H.-P.; Seela, F. Syn-anti conformational analysis of regular and modified nucleosides by 1D ^{1}H NOE difference spectroscopy: A simple graphical method based on conformationally rigid molecules. *J. Org. Chem.* **1990**, *55*, 5784−5790.
(13) Dalpiaz, A.; Townsend-Nicholson, A.; Beukers, M. W.; Schofield, P. R.; IJzerman, A. P. Thermodynamics of full agonist, partial agonist, and antagonist binding to wild-type and mutant adenosine A_1 receptors. *Biochem. Pharmacol.* **1998**, *56*, 1437−1445.
(14) Da Settimo, F.; Primofiore, G.; Taliani, S.; Marini A. M., La Motta, C.; Novellino, E.; Greco, G.; Lavecchia, A.; Trincavelli, L.; Martini, C. 3-Aryl[1,2,4]triazino[4,3-a]benzimidazol-4(10H)-ones: a new class of selective A_1 adenosine receptor antagonists. *J. Med. Chem.* **2001**, *44*, 316−327.
(15) Palczewski, K.; Kumasaka, T.; Hori, T.; Behnke, C. A.; Motoshima, H.; Fox, B. A.; Trong, I. L.; Teller, D. C.; Okada, T.; Stenkamp, R. E.; Yamamoto, M.; Miyano, M. Crystal structure of rhodopsin: a G protein-coupled receptor. *Science* **2000**, *289*, 739−745.
(16) (a) Morris, G. M.; Goodsell, D. S.; Halliday, R. S.; Huey, R.; Hart, W. E.; Belew, R. K.; Olson, A. J. Automated docking using a lamarckian genetic algorithm and an empirical binding free energy function. *J. Comput. Chem.* **1998**, *19*, 1639−1662. (b) Goodsell, D. S.; Morris, G. M.; Olson, A. J. Automated docking of flexible ligands: applications of AutoDock. *J. Mol. Recognit.* **1996**, *9*, 1−5.
(17) Gao, Z.-G.; Chen, A.; Barak, D.; Kim, S.-K.; Müller, C. E.; Jacobson, K. A. Identification by site-directed mutagenesis of residues involved in ligand recognition and activation of the human A_3 adenosine receptor. *J. Biol. Chem.* **2002**, *277*, 19056−19063.
(18) Kim, J.; Wess, J.; van Rhee, A. M.; Schöneberg, T.; Jacobson, K. A. Site-directed mutagenesis identifies residues involved in ligand recognition in the human A_{2a} adenosine receptor. *J. Biol. Chem.* **1995**, *270*, 13987−13997.
(19) (a) Klotz, K.-N.; Lohse, M. J.; Schwabe, U. Chemical modification of A_1 adenosine receptors in rat brain membranes: evidence for histidine in different domains of the ligand binding site. *J. Biol. Chem.* **1988**, *263*, 17522−17526. (b) Olah, M. E.; Ren H.; Ostrowski, J.; Jacobson, K. A.; Stiles, G. L. Cloning, expression, and characterization of the unique bovine A_1 adenosine receptor. Studies on the ligand binding site by site-directed mutagenesis. *J. Biol. Chem.* **1992**, *267*, 10764−10770.
(20) Jiang, Q.; van Rhee, M.; Kim. J.; Yehle, S.; Wess, J.; Jacobson, K. A. Hydrophilic side chains in the third and seventh transmembrane helical domains of human A_{2A} adenosine receptors are required for ligand recognition. *Mol. Pharmacol.* **1996**, *50*, 512−521.
(21) Jacobson, K. A.; Kim, H. O.; Siddiqi, S. M.; Olah, M. E.; Stiles, G. L.; von Lubitz, D. K. J. E. A_3 adenosine receptors: design of selective ligands and therapeutic prospects. *Drugs Future* **1995**, *20*, 689−699.
(22) Rivkees, S. A.; Barbhaiya, H.; IJzerman A. P. Identification of the adenine binding site of the human A_1 adenosine receptor. *J. Biol. Chem.* **1999**, *274*, 3617−3621.
(23) Tucker, A. L.; Robeva, A. S.; Taylor, H. E.; Holeton, D.; Bockner, M.; Lynch, K. R.; Linden, J. A_1 Adenosine receptors-Two amino acids are responsible for species-differences in ligand recognition. *J. Biol. Chem.* **1994**, *269*, 27900−27906.
(24) (a) Javitch, J. A.; Ballesteros, J. A.; Weinstein, H.; Chen, J. A cluster of aromatic residues in the sixth membrane spanning segment of the dopamine D_2 receptor is accessible in the binding-site crevice. *Biochemistry* **1998**, *37*, 998−1006. (b) Marie, J.; Richard, E.; Pruneau, D.; Paquet, J.-L.; Siatka, C.; Larguier, R.; Ponce, C.; Vassault, P.; Groblewski, T.; Maigret, B.; Bonnafous, J. C. Control of conformational equilibria in the human B_2 bradykinin receptor: modeling of nonpeptidic ligand action and comparison to the rhodopsin structure. *J. Biol. Chem.* **2001**, *276*, 41100−41111.
(25) Lin, S. W.; Sakmar, T. P. Specific tryptophan UV-absorbance changes are probes of the transition of rhodopsin to its active state. *Biochemistry* **1996**, *35,* 11149−11159.
(26) Sybyl Molecular Modelling System (version 6.9), Tripos Inc., St. Louis, MO.
(27) Pearlman, D. A.; Case, D. A.; Caldwell, J. W.; Ross, W. S.; Cheatham T. E., III; Debolt, S.; Ferguson, D. M.; Seibel, G. L.; Kollman, P. A. AMBER, a package of computer programs for applying molecular mechanics, normal-mode analysis, molecular dynamics and free energy calculations to simulate the structural and energetic properties of molecules. *Comput. Phys. Commun.* **1995**, *91*, 1−41.
(28) Pearlman, D. A.; Case, D. A.; Caldwell, J. W.; Ross, W. S.; Cheatham T. E., III; Ferguson, D. M.; Seibel, G.; Singh, U. C.; Weiner, P. K.; Kollman, P. A. AMBER 4.1; Department of Pharmaceutical Chemistry, University of California: San Francisco, CA, 1995.
(29) Horn, F.; Weare, J.; Beukers, M. W.; Horsch, S.; Bairoch, A.; Chen, W.; Edvardsen, O.; Campagne, F. G., V. GPCRDB: an information system for G protein-coupled receptors. *Nucleic Acids Res.* **1998**, *26*, 275−279.
(30) (a) Baldwin, J. M. Structure and function of receptors coupled to G proteins. *Curr. Opin. Cell. Biol.* **1994**, *6*, 180−190. (b) Schwartz, T. W. Locating ligand-binding sites in 7TM receptors by protein engineering. *Curr. Opin. Biotechnol.* **1994**, *5*, 434−444. (c) van Rhee, A. M.; Jacobson, K. A. Molecular architecture of G protein-coupled receptors. *Drug Dev. Res.* **1996**, *37*, 1−38.
(31) (a) Xu, W.; Li, J.; Chen, C.; Huang, P.; Weinstein, H.; Javitch, J. A.; Shi, L.; de Riel, J. K.; Liu-Chen, L.-Y. Comparison of the amino acid residues in the sixth transmembrane domains accessible in the binding-site crevices of mu, delta, and kappa opioid receptors. *Biochemistry* **2001**, *40,* 8018−8029. (b) Shi, L.; Simpson, M. M.; Ballesteros, J. A.; Javitch, J. A. The first transmembrane segment of the dopamine D_2 receptor: accessibility in the binding site crevice and position in the transmembrane bundle. *Biochemistry* **2001**, *40*, 12339−12348.
(32) (a) Perlman, J. H.; Colson, A. O.; Wang, W.; Bence, K.; Osman R.; Gershengorn, M. C. Interactions between conserved residues in transmembrane helices 1, 2, and 7 of the thyrotropin-releasing hormone receptor. *J. Biol. Chem.* **1997**, *272*, 11937−11942. (b) Sealfon, S. C.; Chi, L.; Eversole, B. J.; Rodic, V.; Zhang, D.; Ballesteros, J. A.; Weinstein, H. Related contribution of specific helix 2 and 7 residues to conformational activation of the serotonin 5-HT_{2a} receptor. *J. Biol. Chem.* **1995**, *270*, 16683−16688. (c) Zhou, W.; Flanagan, C.; Ballesteros, J.; Konvicka, K.; Davidson, J. S.; Weinstein, H.; Millar, R. P.; Sealfon, S. C. A reciprocal mutation supports helix 2 and helix 7 proximity in the gonadotropin-releasing hormone receptor. *Mol. Pharmacol.* **1994**, *45*, 165−170.
(33) Zhang, D.; Weinstein, H. Polarity conserved positions in transmembrane domains of G-protein coupled receptors and bacteriorhodopsin. *FEBS Lett.* **1994**, *337*, 207−212.
(34) Ryckaert, J. P.; Ciccotti, G.; Berendsen, H. J. C. Numerical integration of the Cartesian equations of motion for a system with constraints: molecular dynamics of *n*-alkanes. *J. Comput. Phys.* **1977**, *23*, 327−333.
(35) Laskowski, R. A.; McArthur, M. W.; Moss, D. S.; Thornton, J. M. PROCHECK: a program to check the stereochemical quality of protein structures. *J. Appl. Crystallogr.* **1993**, *26*, 283−291.
(36) Allen, F. H.; Bellard, S.; Brice, M. D.; Cartwright, B. A.; Doubleday, A.; Higgs, H.; Hummelink, T.; Hummelink-Peters, B. G.; Kennard, O.; Motherwell, W. D. S. The cambridge crystallographic data center: computer-based search, retrieval, analysis and display of information. *Acta Crystallogr.* **1979**, *B35*, 2331−2339.
(37) Head, J.; Zerner, M. C. A Broyden-Fletcher-Goldfarb-Shannon optimization procedure for molecular geometries. *Chem. Phys. Lett.* **1985**, *122*, 264−274.

(38) Gasteiger, J.; Marsili, M. Iterative partial equilization of orbital electronegativity − a rapid access to atomic charges. *Tetrahedron* **1980**, *36*, 3219−3228.
(39) Cornell, W. D.; Cieplak, P.; Bayly, C. I.; Gould, I. R.; Merz, K. M.; Ferguson, D. M.; Spellmeyer, D. C.; Fox, T.; Caldwell, J. W.; Kollman, P. A. A second generation force field for the simulation of proteins, nucleic acids, and organic molecules. *J. Am. Chem. Soc.* **1995**, *117*, 5179−5197.
(40) Dewar, M. J. S.; Zoebisch, E. G.; Healy, E. F.; Stewart, J. J. P. AM1: a new general purpose quantum mechanical molecular model. *J. Am. Chem. Soc.* **1985**, *107*, 3902−3909. (b) MOPAC (version 6.0) is available from Quantum Chemistry Program Exchange, No. 455.
(41) Cheng, Y.; Prusoff, W. H. Relationship between the inhibition constant (Ki) and the concentration of inhibitor which causes 50% inhibition (IC_{50}) of an enzymatic reaction. *Biochem. Pharmacol.* **1973**, *22*, 3099−3108.
(42) Klotz, K.-N.; Hessling, J.; Hegler, J.; Owman, B.; Kull, B.; Fredholm, B. B.; Lohse, M. J. Comparative pharmacology of human adenosine subtypes characterization of stably transfected receptors in CHO cells. *Naunyn-Schmiedeberg's Arch. Pharmacol.* **1998**, *357*, 1−7.

JM049408N